ISTANBUL TECHNICAL UNIVERSITY ★ GRADUATE SCHOOL OF SCIENCE ENGINEERING AND TECHNOLOGY

MULTI RESOLUTION WAVELET ANALYSIS FOR FERRORESONANCE PHENOMENON ON POWER SYSTEMS AND ITS NONLINEAR DYNAMICS

Ph.D. THESIS

Sezen YILDIRIM ÜNNÜ

Department of Electrical Engineering

Electrical Engineering Programme

JANUARY 2015

ISTANBUL TECHNICAL UNIVERSITY ★ GRADUATE SCHOOL OF SCIENCE ENGINEERING AND TECHNOLOGY

MULTI RESOLUTION WAVELET ANALYSIS FOR FERRORESONANCE PHENOMENON ON POWER SYSTEMS AND ITS NONLINEAR DYNAMICS

Ph.D. THESIS

Sezen YILDIRIM ÜNNÜ
(504082006)

Department of Electrical Engineering

Electrical Engineering Programme

Thesis Advisor: Prof. Dr. Ş. Serhat ŞEKER

JANUARY 2015

İSTANBUL TEKNİK ÜNİVERSİTESİ ★ FEN BİLİMLERİ ENSTİTÜSÜ

GÜÇ SİSTEMLERİNDE FERROREZONANS OLAYININ ÇOK ÇÖZÜNÜRLÜKLÜ DALGACIK ANALİZİ İLE İNCELENMESİ VE DOĞRUSAL OLMAYAN DİNAMİKLERİNİN ÇIKARTILMASI

DOKTORA TEZİ

Sezen YILDIRIM ÜNNÜ
(504082006)

Elektrik Mühendisliği Anabilim Dalı

Elektrik Mühendisliği Programı

Tez Danışmanı: Prof. Dr. Ş. Serhat ŞEKER

OCAK 2015

To my family,

FOREWORD

PhD is a very hard work and it is really a long way. I would like to thank my advisor Prof. Dr. Ş. Serhat ŞEKER for his guidence, and his efforts during my PhD studies. I would also like to thank Assoc Prof. Tahir Çetin AKINCI for sharing the necessary power system data.

I was a visiting scholar at Virginia Polytechnic and State University in USA. I would like to express my gratitude to Prof. Dr. Lamine MILI for his support. I was supported by the Scientific and Technological Research Council of Turkey (TUBITAK). If I was not granted for the scholarship, it would be impossible to do the related studies.

I would like to thank to my colleagues Dr. Suna BOLAT, Dr. Lale ERDEM ATILGAN and MSc. Duygu BAYRAM and MSc. Baran ALİKOÇ. They are not only my colleagues but also my beloved friends. It would not be possible to keep on studying without their support.

During my PhD, I did not only learn about my academic interests but I also learnt the value of labor and solidarity. I would like to thank my friends in ITU Research Assistans Solidarity.

There is one person to whom, only thanking would not be enough. As a young, woman scientist I am feeling great gratitude to Mustafa Kemal ATATÜRK. I am following the path he wanted us to follow.

Last but not least, of course it would not be possible to complete my studies without the support of my family. I would like to thank my parents Hatice and Ekrem YILDIRIM for doing everything they can for me to have a very good education. I know education is not the only thing that matters so I would also like to thank my parents for teaching me the value of labor, love and respect. I also would like to thank my sister Melike YILDIRIM for being such an enjoyable person. I also thank my beloved husband Uğur ÜNNÜ for his endless support, friendship and love.

Thanks to Beatles and John LENNON for incredible songs and especially “Imagine.”

November 2014

Sezen YILDIRIM ÜNNÜ
Electrical Engineer, MSc.

TABLE OF CONTENTS

Page

ABBREVIATIONS

CCVT : Coupling Capacitor Voltage Transformer
CRP : Cross Recurrence Plot
CWT : Continous Wavelet Transform
FNN : False Nearest Neighbours
LLE : Largest Lyapunov Exponent
MOV : Metal Oxide Varistor
MRWA : Multi Resolution Wavelet Analysis
ODE : Ordinary Differential Equation
RLC : Resistor, Inductor, Capacitor
SCADA : Supervisory Control and Data Acquisition
STFT : Short Time Fourier Transform
SVM : Support Vector Machine
TEDAŞ : Turkish Electricity Distribution Company
TEİAŞ : Turkish Electricity Transmission Company
TEÜAŞ : Turkish Electricity Generation Company
FNN : False Nearest Neighbours

LIST OF TABLES

Page

LIST OF FIGURES

Page

MULTI RESOLUTION WAVELET ANALYSIS FOR FERRORESONANCE PHENOMENON ON POWER SYSTEMS AND ITS NONLINEAR DYNAMICS

SUMMARY

Power systems are one of the most important infrastructures of a country. The healthy working condition of a power system is crucial. Utilities are making great effort in order to keep the power systems healthy. Nevertheless, it is not always possible to keep these conditions. Power systems face many incidents. As the systems are usually located outdoors, they are very vulnerable to the enviromental effects which can cause serious damage. In addition, the physical parameters of the power system equipment can affect the system operation. Ferroresonance is one of the incidents that power systems might face. It is defined as well as the interaction between the nonlinear inductance and capacitance of the system. In the power system, nonlinear inductance stands for the transformer core and the capacitance is the power line capacitor. Main causes of ferroresonance are short circuits, capacitor switching, transformer switching, insulation faults, lighting, turning the load off suddenly and switching out the transmission line. It is an unpredictable phenomenon and its consequences are destructive. Over voltages, over currents and harmonic frequency components are main results of this phenomenon.

This PhD thesis is focused on identifying the ferroresonance phenomenon and its nonlinear dynamics. In the introduction chapter, the motivation for this study in several studies in the literature is given. Although ferroresonance was studied on power transformers, it is not common to take into consideration all power system component. Previous studies mostly focus on change of transformer parameters. On the other hand, it is not the case on an actual power system as it is not possible to change these parameters. By increasing in the usage of condition monitoring and data collecting systems on power systems, improving new techniques become a necessity. The ferroresonance data are nonstationary and wavelet transform is a powerful tool for analysing this type of data. In this study, the harmonic frequency components are identified by multi resolution wavelet transform in order to interpret related nonlinear dynamics. In addition, related literature survey can be found in introduction chapter.

In the second chapter, theoretical bakcground of ferroresonance phenomenon is described. First, the difference between classical resonance circuits and ferroresonance is described. The equivalent circuits for ferroresonance are given and the phenomenon is described in mathematical manners. Even though ferroresonance is unpredictable, there are numerous approaches for preventing and mitigating the phenomenon. These approaches are also explained in this chapter.

In the third chapter, mathematical methods and signal processing techniques used in this study are explained. Short time Fourier transform, multi resolution wavelet transform and Lyapunov exponents are used for identifying ferroresonance and its nonlinear dynamics. Related mathematical background can be found in this chapter.

In the fourth chapter, the power system modeling is given. The SIMULINK model, and power system parameters are given briefly. The necessary calculations for the equivalent circuit are identified in this chapter.

In the fifth chapter, spectral methods are applied on ferroresonance data. Short time Fourier transform and multi resolution wavelet transform are applied and harmonic frequency components are identified. It is observed that, sub harmonic and quasi periodic harmonic frequency components are created. In addition, phase portraits are constructed in order to understand the evolution of the system.

In the sixth chapter, the largest Lyapunov exponent of the system is estimated. First the dimensions of the system are specified and an estimation method is utilized. As the largest Lyapunov exponent is estimated to be greater than zero, further calculations are applied and by using cross recurrence plots.

In the seventh chapter, nonlinearities calculated by multi resolution wavelet analysis are checked by ordinary differential equations. A new approach for the hysteresis curve is given and it is proven that, the new approach is as useful as the classical approach for modeling the nonlinear curve. The sub harmonic and quasi periodic harmonic frequency components are used as driving force frequencies for differential equations. The phase portraits are plotted seperately and it is proven that, ferroresonance is creating harmonic frequency components.

The detailed comments for outputs and novelties of the thesis are explained in conclusions and discussions chapter.

GÜÇ SİSTEMLERİNDE FERROREZONANS OLAYININ ÇOK ÇÖZÜNÜRLÜKLÜ DALGACIK ANALİZİ İLE İNCELENMESİ VE DOĞRUSAL OLMAYAN DİNAMİKLERİNİN ÇIKARTILMASI

ÖZET

Güç sistemleri bir ülkenin en önemli altyapı bileşenlerindendir. Bu sebeple sağlıklı bir şekilde işletilmeleri çok önemlidir. Güç sistemlerinde oluşan arızalar hem işletmelere büyük ekonomik yükler getirmekte, hem de sisteme bağlı tüketicilerin enerjilerinin kesilmesine sebep olmaktadır. İşletmeler güç sistemlerinin karşılaşması olası arıza durumlarının önüne geçebilmek için yoğun çaba sarf etmektedirler. Güç sistemi içindeki generatörler, transformatörler, kesiciler ve hatta iletim hatları potansiyel arıza noktalarıdır. Sistemde görülen arızalar simetrik (dengeli) ve asimetrik (dengesiz) olmak üzere ikiye ayrılırlar. Arızalar deprem, yıldırım, hayvanlar gibi doğal olaylar ya da bir kapasitenin bozulması gibi sistemdeki ekipmanlarda oluşan hasarlar sebebiyle tetiklenebilir. Her iki durumda da oluşan arızanın hızlı bir şekilde kaldırılması gerekir.

Ferrorezonans güç sistemlerinde nadir karşılaşılan ancak sonuçları yıkıcı olabilen bir durumdur. Sistemdeki doğrusal olmayan endüktans ile kapasite arasındaki etkileşim olarak tanımlanmaktadır. Güç sistemindeki doğrusal olmayan endüktans, doyumlu transformatörlerin çekirdekleridir. Kapasite ise iletim hatlarının uzunluğu nedeniyle oluşan kapasiteler ve kesicilerin topraklama dirençleri nedeniyle oluşan kapasitelerdir. Ferrorezonansın oluşabilmesi için bir gerilim kaynağı ve düşük omik kayıpların olması zorunludur.

Ferrorezonansın sebepleri kısa devre, kondansatör ve transformatörlerin anahtarlama olayları, yalıtım arızaları, yıldırım, yükün aniden devreden çıkması ve iletim hatlarının kopması olarak sıralanabilir.

Ferrorezonans olayının etkileri aşırı gerilimler, aşırı akımlar ve harmonik frekans bileşenleri olarak görülür. Geçici ve sürekli durumlarda görülebilen bu etkiler güç sistemi ekipmanları için zararlı sonuçlar doğurabilir.

Sürekli halde ferrorezonans olayı harmonik frekans bileşenlerine göre dört farklı durum yaratabilir. Bunlar temel durum, alt harmonikler, yarı periyodikler ve kaotik durumlardır. Bu durumlardan biri veya birkaçı sürekli durumda görülebilir ve hangisinin görüneceği sistem parametrelerine ile başlangıç koşullarına bağlıdır. Diğer doğrusal olmayan olaylar gibi, ferrorezonans olayı da başlangıç koşullarına bağlıdır ve sistem parametrelerindeki değişimle ilişkilidir.

Ferrorezonans olayı 1900'lü yılların başından beri incelenmektedir. İlk çalışmalar ferrorezonans olayına grafiksel bir yöntemle yaklaşmış, daha sonra çeşitli analitik yöntemler geliştirilmiştir. Ferrorezonans eş değer devreleri seri veya paralel olabilir. Karmaşık yapıdaki güç sistemlerinin basit bir RLC devresine indirgenmesi ferrorezonans olayının incelenmesini kolaylaştırmıştır.

Ferrorezonans olayı genellikle transformatörler üzerinde incelenmiştir. Ferrorezonansın en önemli sebebinin doğrusal olmayan endüktans olduğu düşünülürse bu şaşırtıcı değildir. Literatürde yapılan çalışmalar genelde transformatörün mıknatıslanma akımı, besleme gerilimi gibi parametrelerinin değiştirilmesi ile ferrorezonansın oluşumu arasındaki ilişkiyi incelemiştir. Buradaki değişimlerin incelenmesinde diferansiyel denklemlerden yararlanılmıştır. Bir RLC devresine indirgenmiş güç sistemi diferansiyel denklemler yardımıyla modellenir. Sistemin doğrusal olmayan özellikleri transformatörün mıknatıslanma eğrisi ile modellenmiştir. Mıknatıslanma eğrisi polinom yaklaşımı ile modellenir ve basit RLC devresi diferansiyel denklemine eklenir. Denklemlerin çözülmesi ile faz protreleri ve çatallanma diyagramları çizdirilir ve böylece ferrorezonansın oluşturduğu sürekli hal durumları incelenir. Ferrorezonansın matematiksel olarak incelenmesi çok önemlidir ancak son yıllarda veri toplama sistemlerinin kullanımının yaygınlaşması ve işaret işleme yöntemlerindeki ilerlemeler de göz önüne alınırsa, işaret temelli yöntemlerin kullanılması kaçınılmazdır.

Bu tez çalışmasında Türkiye enterkonnekte şebekesi içinden seçilen Seyitömer – Işıklar hattında ferrorezonans olayı incelenmiştir. Sistem gerçek parametre değerleri ile Matlab – SIMULINK programında modellenmiş ve yükün aniden kaldırılması ile sistem ferrorezonans çalışmaya zorlanmıştır. Simülasyon üzerinden toplanan gerilim verileri ile ferrorezonans olay tanımlanmaya çalışılmıştır.

Ferrorezonans verileri durağan olmayan verilerdir bu sebeple adi Fourier dönüşümü kullanılması uygun değildir. Ancak mevcut işareti frekans – zaman düzlemine dönüştürebilen Kısa Zamanlı Fourier Dönüşümü (KZFD) kullanılması uygundur. Mevcut gerilim verilerine kısa zamanlı Fourier dönüşümü uygulanmış ve ferrorezonans olayının büyük genlikli yüksek frekansların oluşumuna sebep olduğu görülmüştür. Ancak kısa zamanlı Fourier dönüşümü, büyük genlikli yüksek frekansların varlığını gösterirken, frekans spektrumundaki bileşenlerin hangileri olduğunu gösterememiştir. Bu noktada çok çözünürlüklü dalgacık analizinden yararlanılmıştır. Bu analiz mevcut verinin filtre bankalarından geçirilmesini ve işaretin içindeki frekans bileşenlerinin belirli bir bant aralığında limitlenmesini sağlar. Böylece işaretin içinde var olan ancak görülmeyen özelliklerin ortaya çıkarılması sağlanır. Ferrorezonans verisine çok çözünürlüklü dalgacık analizi uygulanmış ve veri 4 seviyede ayrıştırılma yapılarak incelenmiştir. Bu ayrıştırma sonucunda ferrorezonans öncesinde, güç sistemi temel frekansı olan 50 Hz'lik frekans bileşeni görülmüş ve ayrıca düşük genlikli 100 Hz'lik frekans bileşeni de gözlenmiştir. Güç sistemlerinde ikinci harmonikler dengesizlik anlamına gelmektedir ve burada sistemin sağlıklı çalıştığı durumda bile ferrorezonans olayının oluşmasına sebep olabilecek etkilerin varlığı görülebilir. Çok çözünürlüklü dalgacık analizi sonucunda ferrorezonans sonrası verilerde alt harmonikler ve yarı periyodik harmonikler de gözlenmiştir. Bunlar, 10 Hz, 12.5 Hz ve 25 Hz frekans bileşenleri civarında alt harmonikler, 130 Hz ve 193 Hz civarında ise yarı periyodik harmonik frekans bileşenleridir. Sistemden elde edilen veriler kullanılarak çizdirilen faz portrelerinde de bu frekans bileşenlerinin oluşturduğu düzensiz yörüngeler gözlenmiştir.

Doğrusal olmayan sistemleri incelemek için pek çok yöntemden yararlanılır. Bunlardan birisi de sistemin Lyapunov üstellerinin hesaplanmasıdır. Sistemin en büyük Lyapunov üstelinin değerine göre sistemin kaotik, yarı periyodik veya periyodik bir hareket yaptığı anlaşılır. Temel olarak Lyapunov üstelinin hesaplanması için sistemin başlangıç noktasında birbirine çok yakın iki nokta alınır ve sonlu bir süre boyunca bu iki noktanın birbirlerine göre hareketi incelenir. Eğer aralarındaki mesafe artıyorsa, bu iki yörüngenin birbirinden uzaklaştığı anlamına gelir, bu sıfırdan büyük bir Lyapunov üsteli olup sistemin kaotik bir davranış içinde olduğu anlaşılır. Eğer bu iki noktanın arasındaki mesafe hiç değişmiyorsa bu yarı – periyodik bir harekettir ve bu durumda Lyapunov üsteli sıfırdır. İki nokta arasındaki mesafe azalıyorsa bu durumda da en büyük Lyapunov üsteli sıfırdan küçüktür ve sistemin periyodik bir hareket içinde olduğu anlaşılır. Bir sistemin mertebesi kaçsa, sistemin o kadar sayıda Lyapunov üsteli vardır ama en önemlisi bunların en büyüğüdür. Öte taraftan bu tür bir hesap yapabilmek için sistemin diferansiyel denklemlerini bilmek gerekir. Hatta bu diferansiyel denklemler bilinse bile en büyük Lyapunov üstelinin hesaplanması kolay değildir. Ayrıca güç sistemleri, doğa olayları gibi karmaşık sistemlerde genellikle sistem değişkenlerine ait veriler elde edilebilir ancak bu işaretlerden diferansiyel denklemlere ulaşmak çok kolay olmayabilir. Bu yüzden de en büyük Lyapunov üstelini mevcut zaman serisinden kestirebilmek için çeşitli yöntemler önerilmiştir. Bu yöntemler içinden uygun olan bir algoritma seçilmiş ferrorezonans verilerine ait en büyük Lyapunov üstelinin kestirimi yapılmıştır. Bunun öncesinde sistemin boyutlarının belirlenmesi gerekmiştir. Bunun için Taken tarafından önerilen yöntem kullanılmış, ferrorezonans verisinin altı boyutlu olarak modellenmesi gerektiği anlaşılmıştır. Tercih edilen kestirim yöntemi uyarınca birbirine çok yakın iki noktanın hareketleri ve aralarındaki mesafe kaydedilir ve bu yeni veri grubuna bir eğri uydurulur. Bu eğrinin eğimi en büyük Lyapnuv üstelini vermektedir. Ferrorezonans verilerinin en büyük Lyapunov üsteli sıfırdan büyük ancak sıfıra çok yakın bir değer olarak bulunmuştur. Bu durumda sistemin kaotik bir durumda olduğunu düşünmek gerekir ancak mevcut gerilim verilerinin incelenmesi sonucunda sistemin kaotik bir durumda olmadığı görülmüştür. Bu durumda sadece en büyük Lyapunov üstelinden yola çıkarak bir yorum yapmak sağlıksız olacaktır. Bu durumda doğru yorumlar yapabilmek için başka bir yöntem daha kullanılmış ve sistemin karşılıklı birikim haritaları çizdirilmiştir. Karşılıklı birikim haritaları doğrusal olmayan sistemleri incelerken sıklıkla kullanılan Poincare haritalarının her boyutta çizdirilmiştir şekilleridir. Ferrorezonans verilerine ait karşılıklı birikim haritalarının çizdirilmesi sonucunda sistemin periyodik bir hareket içinde olduğu görülmüştür. Her ne kadar en büyük Lyapunov üsteli sıfırdan büyük olarak hesaplandıysa da karşılıklı birikim haritaları sistemin periyodik bir hareket içinde olduğunu göstermiştir. Lyapunov üstelinin sıfırdan büyük çıkmasına verilerin içindeki gürültüler sebep olmuş olabilir.

Sistemdeki doğrusal olmayan dinamikleri anlayabilmek için basitleştirilmiş eş değer ferrorezonans devresine ait diferansiyel denklemlerin çözülmesi gerekmektedir. Öncelikle ferrorezonans öncesi durum göz önüne alınmış ve RLC devresinin diferansiyel denklemleri çözülmüştür. Diferansiyel denklemin sağ tarafı harmonikli bir kaynakla beslenmiş ve sistemin temel frekansı olan 50 Hz ile ikinci harmonik olan 100 Hz kullanılmıştır. Diferansiyel denklemler çözülmüş ve sisteme ait faz portresi çizdirilmiştir. Ayrıca sistemin faz portresi simülasyondan toplanan verilerle de çizdirilmiştir. Ferrorezonans öncesi durumda sistemin periyodik bir hareket içinde olduğu görülmüştür. Ferrorezonans durum için sisteme doğrusal olmayan endüktansın özelliklerinin eklenmesi gerekir. Normal şartlarda histerisiz eğrisi polinom yaklaşımı ile modellenmektedir ancak trafnsormatörün bu yöntemle modellenebilmesi için gerekli veriler mevcut değildir. Bu durumda polinom yaklaşımının yerine geçebilecek bir yaklaşım aranmış ve histerisiz eğrisini modelleyebilmek için sigmoid fonksiyonundan yararlanılmıştır. Diferansiyel denkleme sigmoid fonksiyon eklenmiş, denklemin sağ tarafı ise harmonik bileşenleri içeren bir kaynakla sürülmüştür. Diferansiyel denklemin çözülmesi sonucunda elde edilen faz portreleri ve sistemden toplanan verilerle çizdirilen faz portreleri karşılaştırılmış ve yeni önerilen diferansiyel denklemin literatürde kullanılan klasik yaklaşım kadar başarılı olduğu görülmüştür. Simülasyon üzerinden alt harmonikler ve yarı periyodik frekanslar ile ilgili veri toplamak mümkün olmamıştır. Öte taraftan yeni önerilen diferansiyel denklem yaklaşımı kullanılarak alt harmoniklere ve yarı periyodik frekans bileşenlerine ait faz portreleri çizdirilmiş ve ferrorezonansın yarattığı sürekli hal durumları ispatlanmıştır.

Bu tez çalışmasındaki en önemli yeniliklerin başında güç sisteminin bir bütün olarak ele alınması gelmektedir. Daha önceki çalışmalarda sadece transformatör dikkate alınırken, bu çalışmada generatörden yüke kadar bütün güç sistemi elemanları dikkate alınmıştır.

İşaret işleme yöntemlerinin kullanılması ile ferrorezonansın yarattığı harmonik frekans bileşenleri belirlenmiş ve bu bileşenler doğrusal olmayan dinamiklerin belirlenmesinde kullanılmıştır.

Literatürde sıklıkla kullanılan bir yöntem olan Lyapunov üstelleri ile sistemin davranışını incelenmiş ancak bu yöntemin tek başına tam olarak sağlıklı sonuç vermediği görülmüştür. Burada yapılacak iki çalışma vardır. Öncelikle kullanılan zaman serisinin simülasyon gürültüsünden temizlenmesi gerekir. İkinci olarak ise en büyük Lyapunov üstelinin kestirimi için kullanılacak yöntemin değiştirilmesi önerilebilir.

Literatürde sıklıkla kullanılan bir yöntem olan histerisiz eğrisinin polinom yaklaşımı ile modellenmesinin yerine sigmoid fonksiyon kullanılması önerilmiş, bu fonksiyonun da geçerliliği diferansiyel denklemlerin çözülmesi ve sisteme ait faz portrelerinin çizdirilmesi ile ispatlanmıştır.

Gelecekte yapılacak çalışmalarda en önemlisi gerçek bir güç sistemi verisi üzerinde ferrorezonansın etkilerinin incelenmesi ve tez çalışmasında önerilen yöntemlerin gerçek zamanlı bir veri üzerinde geçerliliğinin incelenmesidir. Ayrıca diferansiyel denklemleri gerçekleyen bir analog devre modelinin kurulması da gelecekte yapılacak çalışmalar arasındadır.

1. INTRODUCTION

The healthy operation of power systems is very important therefore utilities are making a huge effort on ensuring the robust operating conditions of these systems. Nevertheless, power systems struggle with numerous faults from generation side to distribution side. Generators, transformers, electrical machines, circuit breakers and even the transmission lines are potential fault locations on power systems. The faults in power systems cause many economic damages. Some faults might be fatal and the consequences might be destructive. As a result, many customers might be out of power.

The faults on power systems can be classified as:

- Symmetrical (balanced)
- Asymmetrical (unbalanced) [1].

The faults might be triggered by natural events like an animal, lightning etc. or might be triggered by the failure of power system equipment like a capacitor. In either case, the fault should be cleared rapidly.

One of the consequences of a power system fault is ferroresonance which is a nonlinear phenomenon. The results of the ferroresonance might be destructive. It is a jump resonance and is explained as the interaction between a nonlinear inductance and a capacitance. The nonlinear inductance, which is a consequence of saturable ferromagnetic material of the transformer core, is defined as the magnetizing inductance of transformers. The capacitance of long transmission lines and the grounding resistance of circuit breakers are the main capacitances of a system. A voltage supply and low ohmic system losses are also mandatory for the occurrence of ferroresonance phenomenon [2–4].

Occurrence of ferroresonance is dependent on the abnormalities of the power system. Main causes are short circuits, capacitor switching, transformer switching, insulation faults, lightning, turn off the load off suddenly and switching out the transmission line [3, 5, 6].

Ferroresonance is an unpredictable phenomenon and its identification is also a difficult process. If a system faces:

- high permanent over voltages,
- high permanent over currents,
- high permanent distortions of voltage and current waveforms,
- displacement of the neutral point voltage,
- transformer heating (in no-load operation),
- continuous, excessively loud noise in transformers and reactances,
- damage of electrical equipment (capacitor banks, VT, ...) due to thermal effect or insulation breakdown,
- apparent untimely tripping of protection devices,

it is possible to refer to ferroresonance but these conditions are not enough as they might be the conclusions of other abnormal situations like short circuit. There should also exist other qualifications of the system like:

- simultaneous presence of capacitances with non-linear inductances,
- existence of at least one point whose potential is not fixed in the system (isolated neutral, single fuse blowing, single phase switching....),
- lightly loaded system components (unloaded power or instrument voltage transformers...) or low short-circuit power sources (generators).

If one or more of the above are observed in the system, it is possible to identify the ferroresonance. [3]

The results of ferroresonance are over voltages, over currents and harmonic frequency components [7–9]. Transient and steady state harmonic frequency components are dangerous for the equipment of power systems [10].

There are four types of steady state behavior of a power system with ferroresonance.

Fundamental Mode: In this mode of ferroresonance, the outcoming overcurrent or overvoltage waves contain harmonic frequency components which are periodic with the fundamental frequency (f_0) of the system i.e. $2f_0$, $3f_0$...

Sub-harmonic Mode: The outcoming waves are constituted of the fundamental frequency (f_0). Harmonic frequency components with frequencies f_0/n are seen where n is an integer.

Quasi-periodic Mode: The outcoming waves are not periodic with the fundamental frequency (f_0). On the other hand, the resultant waves consist of frequencies nf_1+mf_2 where n and m are integers and f_1/f_2 is an irrational real number.

Chaotic Mode: The obtained waveforms are non-periodic and there is not a certain rule for the frequency components [3].

The system may involve one or more of these steady state behaviors. The steady state behaviour depends on the initial conditions of the system.

The nonlinear inductance, which is represented by the transformer in power systems, is the main reason for occurrence of ferroresonance. Therefore, research mostly focuses on the transformer modeling and its effects on ferroresonance; the effects of the change in the slope of the hysteresis curve, the change of magnetizing resistance (R_{fe}), and the impact of the magnetic couplings in three phase transformers are investigated. Bifurcation diagrams and Poincare maps are utilized in order to understand the effects of these changes [11–16]. Change of the supply voltage also affects the ferroresonance and the observed ferroresonance steady state mode [11, 13, 17].

Ordinary differential equations (ODE) are a common tool for modeling the behavior of ferroresonance circuit. The differential equation for the equivalent resistor, inductor and capacitor (RLC) circuit is sufficient to model the stable and non-stable modes of ferroresonance. The nonlinear inductance is traditionally modelled by a polynomial function [18, 19]. Harmonic balance method and Galerkin method are utilized for solving the ODEs. Harmonic balance method is suitable for periodic solutions and Galerkin method is suitable for boundary value problems [20–24].

Nonlinear dynamics and especially bifurcation diagrams are commonly used for identifying ferroresonance. Bifurcation is brought into the literature of nonlinear dynamics by Henri Poincaré. It is used for identifying the change of a characteristic of the observed system by varying one or more parameters [25]. By solving the differential equations for varying parameters of the system, it could be possible to define the stable and unstable operating conditions of the system as well as the obtained ferroresonance modes [26]. In order to plot the bifurcation diagrams of the system, either the differential equations should be solved or the experimental data should be used. The bifurcation parameter can be any system parameter. As nonlinear iron core is the main cause of ferroresonance, the relationship between the core and input voltage, i.e. source voltage, the capacitance value of the system and the change of the opening instance of circuit breakers are widely studied [7, 8, 27–30]. Bifurcation studies are also strictly related with the impacts of change in initial conditions studies.

Although, ferroresonance in power transformers was broadly studied, the studies related to the whole power system are very limited. These studies are usually case studies and they cannot give brief information about the nature of ferroresonance [31, 32]. If the whole power system is modelled it would be possible to understand the effects of system parameters on ferroresonance. The use of supervisory control and data acquisition (SCADA) systems for power systems is scaled up. As data collecting becomes easier, the researchers focused on signal processing techniques. Wavelet analysis is mostly used for identifying the ferroresonance. The main idea is to decompose the signal into its frequency components and extract the related features of ferroresonance. These studies focused on the sub harmonic frequency band and identified 2^{nd} and 3^{rd} sub – harmonics. Also neural networks are utilized for identifying the ferroresonance [10, 33–37]. On the other hand, identifying the ferroresonance is not adequate. Over voltages and frequency components can be consequences of other power system abnormalities like short circuit. For classification of ferroresonance, soft computing tools like fuzzy logic and neural networks are used [25, 36, 37]. Although the use of soft computing tools is proposed, it should be noted that, for big power systems development of more reliable techniques is a necessity. S –Transform, which is a generalized short time Fourier transform with continuous wavelet transform, and a new machine learning system called support vector machine (SVM) are also proposed. As SVM depends on the statistical variations of the signal, it is a more robust technique for classifying ferroresonance [8, 27].

The main motivation of this thesis is to clearly identify the harmonic frequency components that ferroresonance generate and identify the nonlinear dynamics related with the phenomenon. Previously, continuous wavelet transform (CWT) was utilized in order to classify the happening of ferroresonance [10, 38]. But CWT was not successful to clearly point out the exact frequency components as desired. Ferroresonance data are usually non stationary, i.e. multi frequency components are involved, so wavelet transform is a suitable tool for processing. Provided that the signal is limited into certain frequency bands, the precise frequency components can be calculated. Short time Fourier transform (STFT) and multi resolution wavelet transform (MRWA) are used for identifying the harmonic frequency components of the system. These harmonics can be used to define the nonlinear behavior of the system. Sub – harmonics and quasi periodic harmonics are associated with the nonlinear behaviors of the electrical system.

This thesis is divided into eight chapters including the introduction. In Chapter 2, the ferroresonance phenomenon is explained in an analytical approach. The difference between resonance and ferroresonance is defined. Moreover the steady state behavior of ferroresonance is investigated. Analytical approach to ferroresonance is deeply identified via mathematical equations. The methods for preventing and mitigating ferroresonance are also described.

In Chapter 3, the mathematical methods used within the thesis are explained. Short time Fourier transform, multi resolution wavelet transform, Lyapunov exponents are explained in mathematical manners.

In Chapter 4, the power system used for the ferroresonance studies is explained. The system parameters are given. The SIMULINK model and the equivalent circuits for the generator,the transformer and the power line are described in details.

In Chapter 5, the simulation steps are described. STFT and MRWA are applied to the voltage data collected from the simulation and related outcomes are achieved from frequency – time domain. The steady state of the ferroresonance is investigated.

In Chapter 6, a Lyapunov exponent estimation method is applied for ferroresonance data. The attractor is reconstructed and the largest Lyapunov exponent is estimated. Also recurrence plots are generated and related comments are given.

In Chapter 7, the differential equation for a RLC circuit is derived. First, a linear RLC circuit is considered for the pre – ferroresonance region and phase portraits are constructed. Then a sigmoidal function is added to the differential equation in order to simulate the nonlinear inductance. In this case, the phase portraits are constructed for three different situations which are; fundamental, sub harmonic and quasi periodic ferroresonance.

In the discussions and conclusions chapter, the outcomes are summarized. Signal processing methods and their importance on power system modeling are reviewed. Advantages and disadvantages of the proposed method about nonlinearities are presented. The future works are also discussed in this chapter.

2. THEORETICAL BACKGROUND OF FERRORESONANCE PHENOMENON IN THE LITERATURE

The ferroresonance phenomenon has been studied for over a hundred years. The first studies were done by Joseph Bethenod in 1907 about the resonance in transformers. On the other hand, the word “ferroresonance” first appears in the literature in 1920 by Paul Boucherot. Boucherot analyzed the phenomenon through a circuit which is built up with a resistor, a nonlinear inductor and a capacitor. Two stable fundamental frequency operating points were observed through the series circuit [39, 40]. Ferroresonance became a serious problem in 1930s, when series capacitors were utilized in order to improve the voltage regulations distribution systems [39, 41].

The first graphical approach for ferroresonance was explained by Rudenberg in 1940s. [39, 42]. Rudenberg explained the jump characteristic of ferroresonance by analyzing the operating point of the circuit regarding to the change of capacitor charging current. The main foible of this approach is that it only takes cognizance of the fundamental ferroresonance and neglects the harmonic components.

Studies were carried out regarding the transformer modeling and ferroresonance as a system later based on Hayashi’s studies [39].

Although ferroresonance is still a resonance circuit, its behavior is different from the basic resonant circuit. In physical means, a periodically driven system oscillates with a certain frequency. If the frequency of this oscillation is equal to the natural frequency of the system, the amplitude of the oscillations tend to get larger. As a result, after excessing a certain amplitude, the system cannot preserve the healthy situation and it collapses. Electrical resonance is formed if the inductive and capacitive reactances of a circuit are equal to each other. Resonance circuits can be either series or parallel. In Figure 2.1 simple resonance circuits are shown. The calculation of the resonance frequency is given in Equations 2.1 and 2.2.

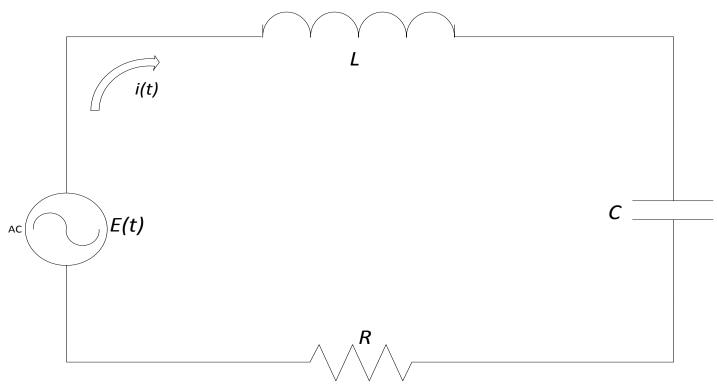

(a)

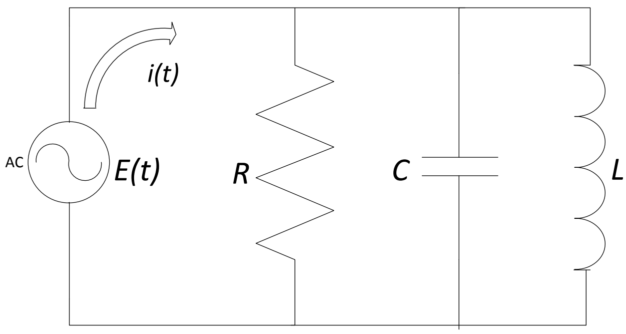

(b)

Figure 2.1 : Resonance circuits a) Series. b) Parallel.

$$\omega L = \frac{1}{\omega C} \qquad \textbf{(2.1)}$$

$$f_s = \frac{1}{2\pi\sqrt{LC}} \qquad \textbf{(2.2)}$$

Where f_s stands for the fundamental frequency of resonance circuit [43 - 44]. In Figure 2.2 the flux – current (φ-I) characteristic of a linear inductance and the frequency response of a RLC circuit are shown [17].

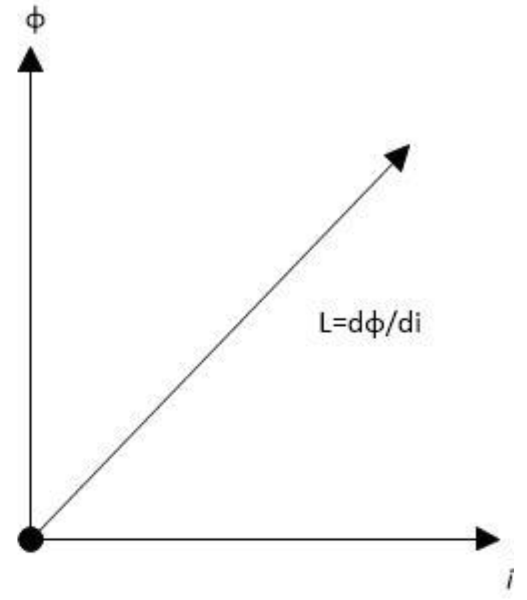

(a)

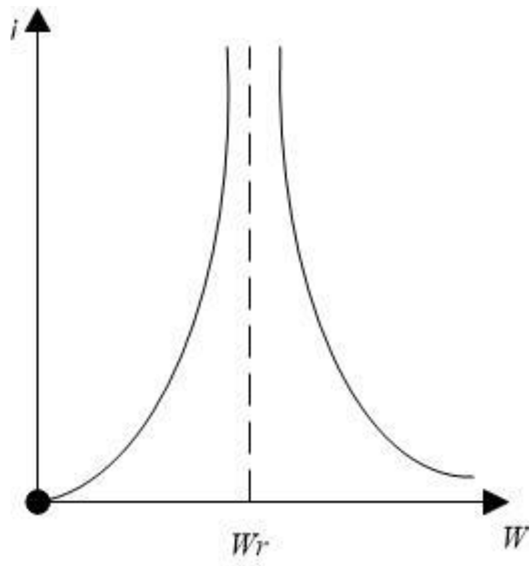

(b)

Figure 2.2 : a) The φ-I characteristic of a linear inductance. b) Frequency response of a RLC circuit.

On the other hand, as it was previously stated, ferroresonance circuits, i.e. nonlinear resonance, circuits consist of a nonlinear inductance. The phenomenon can not only be defined with a single frequency, but also with the magnetic flux of the iron core, i.e. the transformer. [41]. In Figure 2.3 the φ-I characteristic of a nonlinear inductance is given. It is clear that the characteristic is similar to the hysteresis curve of a transformer. For the linear part of the characteristic, the system will not face any problems but the transformers operate mostly at the knee point. With any disturbance, the transformers may drift to the saturation region and ferroresonance may occur under these circumstances.

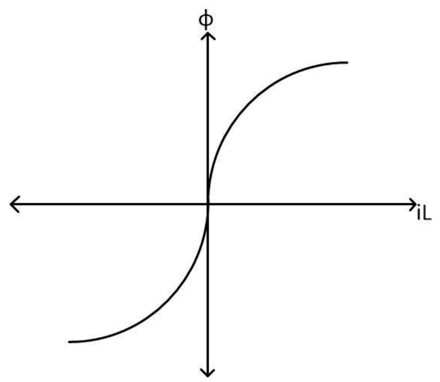

Figure 2.3 : The φ-I characteristic of a nonlinear inductance.

Ferroresonance circuits are divided into two types;

- Series or parallel circuits
- Mono phase or three phase circuits [2] .

An RLC equivalent circuit of the system is sufficient in order to model the ferroresonance. In Figure 2.4 an equivalent circuit for ferroresonance is given. It is clear that, the inductance is modelled as a nonlinear inductance.

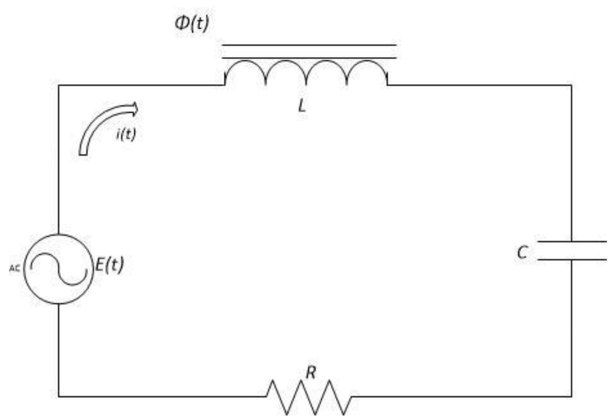

Figure 2.4 : An equivalent RLC cirucit for ferroresonance.

Mathematical modeling of the circuit is based on several physical parameters and a nonlinear differential equation is utilized. The relationship is given in Equation 2.3.

$$\frac{dx}{dt} = F\ (x, t, \beta) \qquad \textbf{(2.3)}$$

where x stands for state variables like current and β stands for the physical parameters like the length of the transmission lines, impedance values [6].

There are two main characteristics of ferroresonance which are;

- Sensitivity to system parameters,
- Sensitivity to initial conditions [3, 45, 46],

The latest research focuses on the effects of these characteristics on the system. In order to analyze the system's sensitivity to the change of parameters, the researchers defined the most important parameters that are influencing ferroresonance. The parameters affecting ferroresonance are;

- Supply voltage
- System capacitance
- Either primer or magnetizing resistances of the transformer
- Hysteresis curve
- Circuit breakers opening instant or their grading capacitances.

The most important system parameter is the hysteresis curve of the transformer because it identifies the nonlinear core itself. The hysteresis curve of a nonlinear core is best described by the Preisach Theory, which states that all ferromagnetic materials are made up small dipoles [11]. The change in the hysteresis curves affects the hysteresis and iron core losses of the transformer. The losses are proportional to the area of the closed loop. As the curve gets wider, the losses will get higher, thus the possibility of the occurrence of ferroresonance will be reduced [12]. Changing the slope of the hysteresis curve slightly, effects the time domain waveforms ,i.e. φ-$d\varphi$ phase planes, dramatically [13]. On the other hand, while having the same amount of losses with different hysteresis curves for a nonlinear inductance, the observed ferroresonant modes are different from each other [14]. Also, the magnitude of the magnetizing resistance (R_{fe}) of the transformer affects the occurrence of ferroresonance. Lower magnitude of the resistance leads to lower losses and prevents ferroresonance [15].

Change of the supply voltage is an other important system parameter. Changing the amplitude of supply voltage affects the transformer and leads it into the saturation region. Depending on the amplitude of supply voltage, it is possible to see bifurcations. The system may face different types of ferroresonance [17]. Depending on the percentage of the change, the system may shift from a stable mode to an unstable mode [13]. Lower levels of the supply voltage than the nominal voltage cause sub harmonic oscillations [11].

While explaining the sensitivity to system parameters, it is a good opportunity to explain the jump resonance too. In Figure 2.5 the graph stands for the inductance voltage (V_L) vs. the amplitude of source voltage (E) [3]. It is obvious that the system has only one stable point for $E=E_1$. For $E=E_2$ the system has two stable and one unstable points. For $E=E'_2$, the system suddenly jumps from one stable point to another. This is called jump resonance. M_2 and M_1 are bifurcation points of this system. Investigations around these points may lead the researchers to understand the steady state behaviour of ferroresonance.

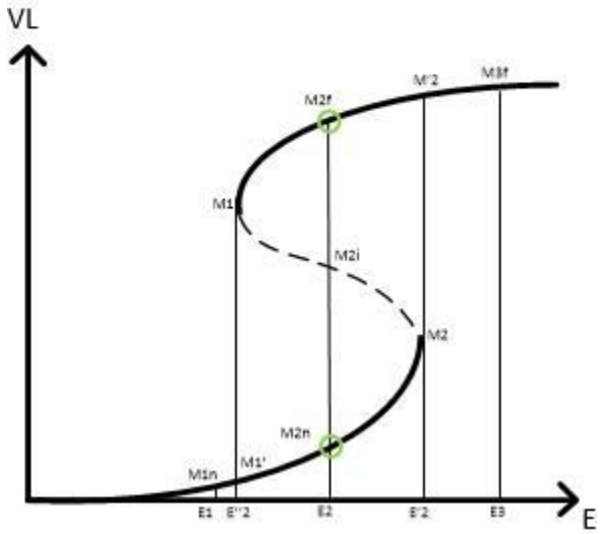

Figure 2.5 : The V_L – E characteristic of a basic ferroresonance circuit.

The opening instants of circuit breakers for the identical values of flux of transformer do not affect the occurrence of ferroresonance or its modes but affect the phase plane trajectories. It is clear that the initial conditions should be chosen correctly [13]. On the other hand, if the opening instant of the circuit breaker affects the transformer flux, it is obvious that the occurrence of ferroresonance and its stable modes will be influenced [47].

Sensitivity to initial conditions is a crucial characteristic for all nonlinear systems. Ferroresonance is not an exemption. The same system can behave different for different initial conditions. For ferroresonance research, the studies mostly focused on the changes of supply voltage (E) and transformer flux (φ) [45, 48, 49]. The research related to the transformer losses pointed out that, in a power system modeling transformer losses should not be neglected. Neglecting or assuming the losses very low, causes misinformation regarding to the steady state of ferroresonance. If a transformer is modelled with the real loss parameters, it faces a chaotic ferroresonant mode whereas neglecting the losses of the same transformer leads the researcher into facing fundamental and quasi-periodic modes [18, 50]. Related research concluded that, the change of initial conditions had a great impact on the steady state modes of the ferroresonance. In Figure 2.6 a representational graph for different initial conditions of the same system is given. The same system starting with different initial conditions ends up with different steady states [3].

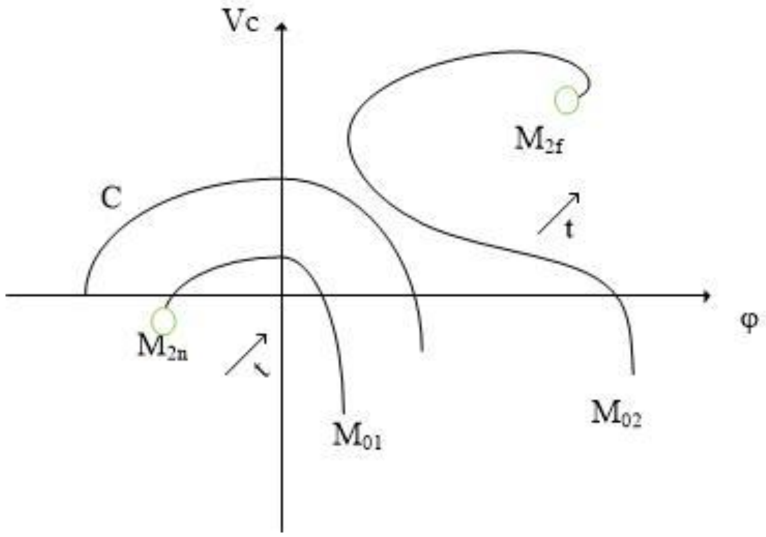

Figure 2.6 : A representational graph for different intial conditions.

2.1 Analytical Approach to Ferroresonance

It was previously stated that the equivalent circuit for ferroresonance is either a series or a parallel RLC circuit. A RLC circuit can easily be modeled with differential equations. But it should be noted that, for ferroresonance modeling, the effect of the nonlinear core should not be omitted. The flux – current characteristic of the transformer is defined in Equation 2.4. α and β are the coefficients related with the hysteresis curve of the transformer, where α stands for the linear region and β stands for the nonlinear region. For modern transformers, n is chosen as high as possible but research shows that, a value between 3 - 7 is sufficient to model the transformer. Φ is the flux of the transformer [18].

$$i_{m=} \alpha\phi + \beta\phi^{n} \quad \textbf{(2.4)}$$

The basic differential equation for the nonlinear circuit is given in Equation 2.5 [18 - 19].

$$\frac{d^2\phi}{dt^2} + \frac{1}{RC}\frac{d\phi}{dt} + \frac{1}{C}(\alpha\phi + \beta\phi^n) = \omega E cos(\omega t) \quad \textbf{(2.5)}$$

Here,

Φ stands for the flux of the circuit, ω stands for the angular frequency and E stands for the supply voltage.

A first order solution for Equation 2.5 is given in Equation 2.6.

$$\Phi(t) = a\cos(\omega t) + b\sin(\omega t) \quad \textbf{(2.6)}$$

This solution is used for the harmonic balance method, which is a very popular method for solving nonlinear differential equations. This method states that, every state variable of the system is modelled by Fourier series. The coefficients of the Fourier series should be tuned carefully by using a proper optimization algorithm for achieving the least error. The main difficulty for this method is that the number of coefficients that should be tuned is very extensive so a method for eliminating the coefficients for very large systems should be addressed [20]. Galerkin method is also very useful for solving boundary value problems. Harmonic balance method solves the steady state response of the system and finds the periodic solutions whereas Galerkin method solves boundary value problems. The main approximations are similar, assuming Fourier series as a solution of the system [21 – 24].

Early research for analytical approach of ferroresonance focused on solving the nonlinear differential equation of the system for different system parameters. The jump characteristic of the ferroresonance was explained by the change of the parameters [51–53]. Main problem with these early studies was that, they were only considering the fundamental ferroresonance. The other harmonic components were neglected.

Newer research for analytical solution of ferroresonance proposes different approximations for faster and more reliable calculations. For an easier calculation, a method to replace the nonlinear ODE with linear constant coefficient ODE is proposed [19]. According to this method, the nonlinear inductance is modelled in two regions, i.e. saturated and unsaturated regions. The flux linkage equation for nonlinear inductance is modelled. The nonlinear ODE is then rewritten with that equation and it is stated that, by changing the L value, the transient behaviour of ferroresonance is achieved. This research also sought for the relationship between the open phase angle of circuit breaker and the saturation of the iron core. It concluded that they are strictly related. Also the natural response of the differential equation is more related with ferroresonance than the forced response. By using the two segment magnetizing characteristic of the nonlinear iron core, a new V-I characteristic for the nonlinear core is analytically calculated. Although this method only takes the fundamental ferroresonance into account, the obtained V–I characteristic can be manipulated with varying frequency values for ferroresonance [54, 55].

2.2 Preventing and Mitigation of Ferroresonance

Although the conditions affecting the occurrence of ferroresonance are determined widely, it is still a highly unpredictable phenomenon. There are important points that the operators should take care of for preventing the sparking ferroresonance. These are:

- Avoiding single-pole switching in three phase systems.
- Avoiding open circuit or low load operations of transformers.
- Proper design of switching operations [3, 28].

In order to prevent ferroresonance, the design of the system is also critical. In the system design stage, the circuit parameters should be chosen carefully. One of the most fatal components of ferroresonance is the transformer connection type. The connections with ungrounded primary windings of the transformer are more inclined to ferroresonance than the others. In Table 2.1. these connections are shown [29]. On the other hand, it should be noted that not only the transformer connections can force the occurrence of ferroresonance. If the system parameters are not chosen in the area of risk, ferroresonance does not occur [3, 29].

Table 2.1 : The transformer connection types which lead to ferroresonance.

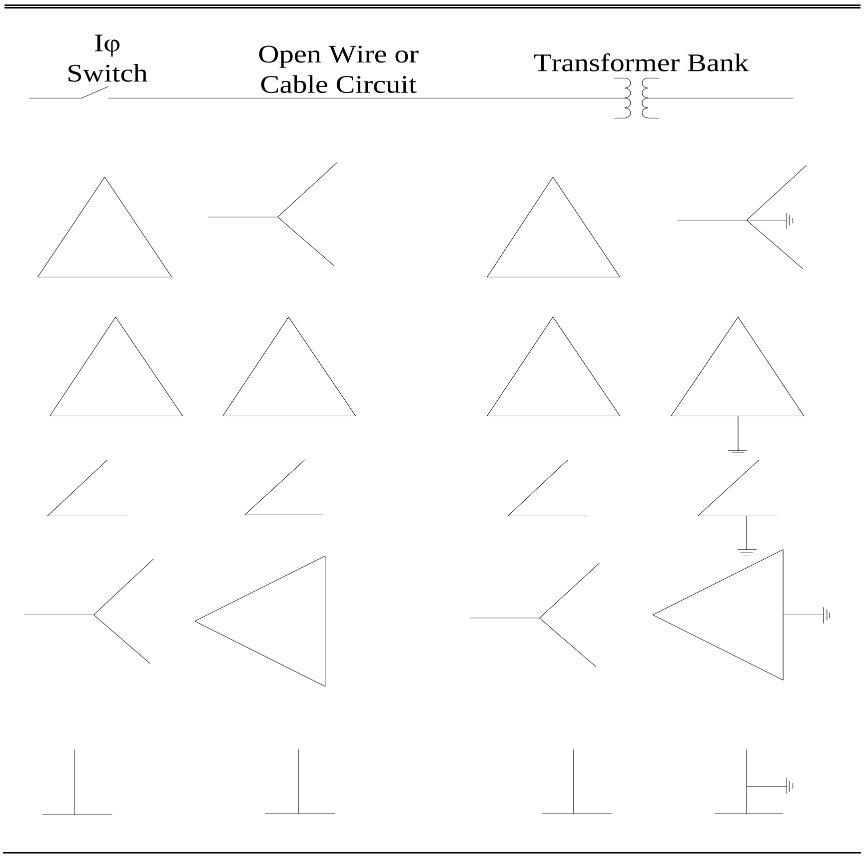

The other factors affecting ferroresonance are;

- The existence of phase to phase or phase to ground capacitances between the single-pole switches and transformer,
- An efficient grounding of the generator side [29].

Carefully selecting the transformer connection types and their grounding will be very effective in preventing ferroresonance.

The second critical design point is the selection of transmission lines. As it was previously stated, long lines are the main supply of the system capacitance. If there exists a suitable condition, these lines may interact with the nonlinear inductance and cause ferroresonance [7].

The consequences of ferroresonance might be destructive, so mitigating ferroresonance is a crucial problem. The most common ways suggested for suppressing the ferroresonance are adding a series resistor or a saturable reactor to the secondary windings or adding an air-core reactor parallel to the primer windings of the transformer [3, 30]. The use of damping resistance is the most basic way. The value of the damping resistance is given in Equation 2.7 [30].

$$R = K\sqrt{\frac{L}{C}} \qquad \textbf{(2.7)}$$

The value of K determines whether the system is critically (K=1/2), under (K<1/2) or over (K>1/2) damped [30]. According to system parameters, the most suitable value for damping resistance can be calculated. The same paper also concludes that, in order to add a resistance in series to the circuit, adding a group of resistances in parallel and disconnecting them step by step is a more efficient way for damping the ferroresonance.

On the other side, the damping resistance might cause some thermal problems during other faults like single phase-earth faults [56]. Adding a saturable core reactor to the secondary windings is a way to both damp ferroresonance and prevent thermal damage. The reactor adds more loads in case of the occurrence of over voltages [57, 58]. Under normal operating conditions, the current through this reactor is imperceptible. Also the effects of the core to the transients are very less. This approach was used for the USA Amtrak train company [59]. It is a very convenient way for high voltage power transformers. In order to settle a decent damping load, a control unit is also vital. The unit might be designed by microprocessors and power electronics switching elements in order to tune the corrects damping load [56, 60].

A very basic but efficient ferroresonance suppression device is a filter bank. As ferroresonance is related to the harmonics, a filter around the fundamental frequency of the system can be designed in order to damp the ferroresonance. In Figure 2.7 various filter types are shown. The filter blocks the fundamental frequency and passes other frequency components to the damping load [57]. However, this method is mostly used in coupling capacitor voltage transformers (CCVT), which are used for monitoring, measurement and protection [61].

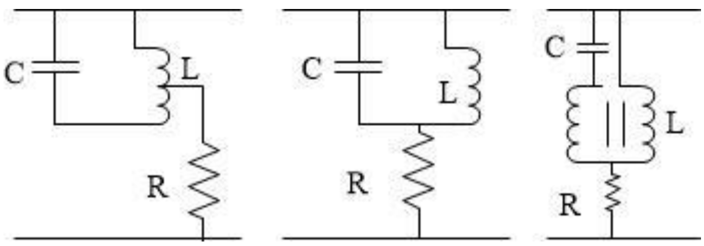

Figure 2.7 : Various filter types for ferroresonance damping.

Power electronics devices have gained importance in control circuits, thus they are also important for ferroresonance suppression devices. Surge arresters are the main devices used against over voltages and sparks in power systems [62]. Metal oxide varistors (MOV) are used in power systems against over voltages. In Figure 2.8 the equivalent circuit of a MOV is given where L is the inductance of conducting leads and C is the total capacitance of the MOV [62]. An appropriate modeling of the MOV is added to the dynamical model of the power system and simulations conclude that a MOV can damp the chaotic over voltages caused by ferroresonance. Although MOVs are reliable and have stable characteristics the main concern is that the amount of power that MOVs can deplete is very limited [57, 62, 63].

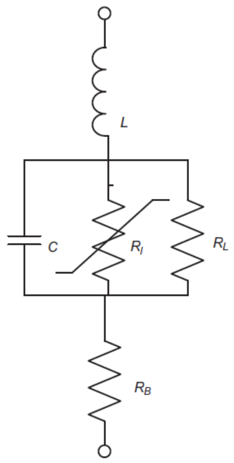

Figure 2.8 : The equivalent circuit of a MOV.

In a different study, a method is proposed for controlling the power on the damping resistor by power electronics circuits [58]. By using thyristors, a chopper circuit is built. For triggering the thyristors, a 1.4 p.u. of over voltage is chosen. The simulations demonstrate that, the chopper circuit is more efficient than a fundamental frequency blocking filter and saturable reactor.

3. MATHEMATICAL METHODS

This chapter is devoted to the mathematical methods related to the data processing and analytical approach to the ferroresonance phenomenon. Short time Fourier transform, multi resolution wavelet transform and Lyapunov exponent calculation will be explained in mathematical manners.

3.1 Short Time Fourier Transform

Fourier transform is widely used for extracting the frequency components of a signal. Fourier transform is suitable for signals that are periodic with an infinite duration. On the other hand, Fourier transform cannot give information about the time – frequency components. For overcoming this problem, in 1946 Gabor introduced windowed Fourier transform also known as short time Fourier transform. In Equation 3.1, STFT is given in integral form for continuous signals.

$$STFT_f(\omega,\tau) = \int_{-\infty}^{\infty} g(t-\tau)f(t)e^{-j\omega t}dt \tag{3.1}$$

Here;

g(t-τ) stands for the window function which is chosen by the user, *t* is time and *w* is the frequency. Gaussian, Hamming, and Hanning are popular rectangular window functions. STFT transforms one variable function to two - variable function which are time and frequency. The disadvantage of STFT is either a good time resolution or frequency resolution can be achieved. This is the result of constant window size. In Figure 3.1 the illustration regarding to the resolution is given [64 – 67].

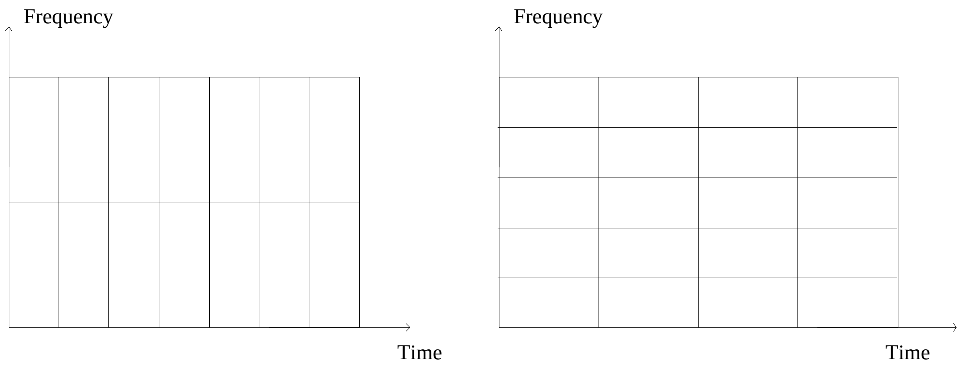

Figure 3.1 : Comparison of the STFT resolution.

Spectogram is the squared magnitude of STFT and gives the energy distribution of the transform. It is given in Equation 3.2.

$$S(w,\tau)=|STFT(w,\tau)|^2 \quad \textbf{(3.2)}$$

3.2 Multi Resolution Wavelet Analysis

Wavelet transform is basically used for identifying the localized feature in time – frequency domain. Although STFT is also a two variable transform, the size of the window function is fixed. On the other hand, if it was possible to change the window size, it would be possible to better identify time of frequency information. Wavelets are first introduced by Haar in the early 1900s as an alternative to the Fourier transform. Until 1980s, there was not a significant progress in wavelet transform but in 1980s, Morlet's research related to continuous wavelet transform brought an acceleration to the study field. Since then, many researchers like Meyer, Daubechies, Mallat and Akansu studied wavelet transform [33, 68 – 70].

Wavelet transform enables the change of the window size. Long time periods for low frequency information and short time periods for high frequency information can be used [71]. In Figure 3.2 the time – frequency resolution of the wavelet transform is given.

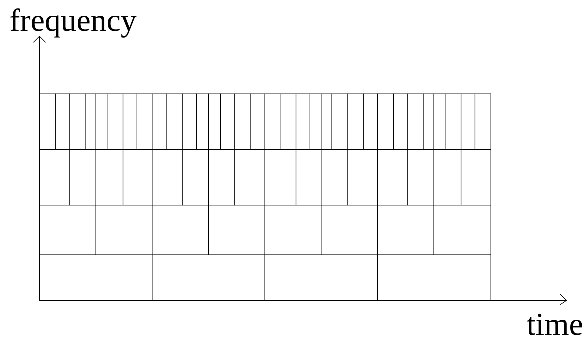

Figure 3.2 : Time –frequency resolution of wavelet transform.

In Equation 3.3 continuous wavelet transform is given.

$$W_s(a,b) = \frac{1}{\sqrt{a}} \int_{-\infty}^{\infty} s(t) h * \left(\frac{t-b}{a}\right) dt \qquad \textbf{(3.3)}$$

Where,

h(t) is the mother wavelet. Daughter wavelets are derived from the mother wavelet. Daughter wavelets are given in Equation 3.4.

$$h_{ab}(t) = \frac{1}{\sqrt{a}} h(\frac{t-b}{a}) \qquad \textbf{(3.4)}$$

where,

a is the scale parameter,

b is the translation parameter.

Translation parameter is used to change the center of a localized wavelet function. As the scale parameter a changes, the daughter wavelets will change too. $1/\sqrt{a}$ is a normalizing coefficient which is used to have a constant energy of the signal [72].

Continous wavelet transform generates many redundant data. For overcoming this problem, Ingrid Daubechies created discrete wavelets. In Equation 3.5 the wavelet function with discrete parameters is given.

$$h_{jk}(t) = \frac{1}{\sqrt{a_0^j}} h\left(\frac{t - kb_0 a_0^j}{a_0^j}\right) \qquad \textbf{(3.5)}$$

Where;

a = a_0^j; $a_0 = 2$;

b = $b_0 a_0^j$; $b_0 = 1$

j and k are integers [73, 74].

Discrete wavelets are used for Multi Resolution Wavelet Transform (MRWA) which is a discrete transform. The main idea for MRWA is splitting the signal into low frequency and high frequency bands. Basically, low pass and high pass filters are used.

Vector spaces are the basic structures of MRWA. All vector spaces with lower resolution are spanned by a higher resolution vector space. The basis of each vector space is the scale function for wavelet. The properties of MRWA are [65, 74];

- an(t) = a (t-n) forms an orthonormal basis for V0
- Vm = DmV0
- Vm+1 ⊂ Vm

In Figure 3.3 the representation of MRWA is given.

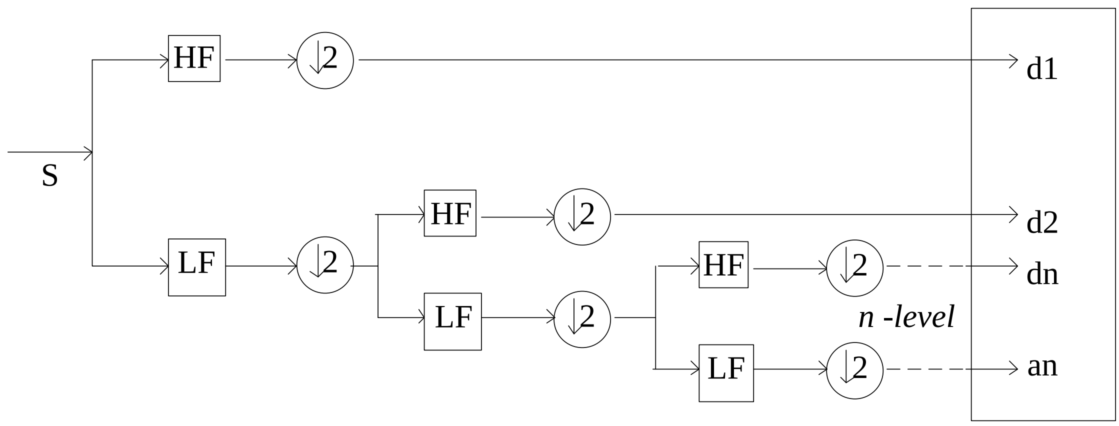

Figure 3.3 : Decomposition diagram for an n level MRWA.

In MRWA, High frequency components are named as details (d_n) and low frequency components are named as approximations (a_n). In every decomposition level, the signal is down sampled by 2.

3.3 Lyapunov Exponent Calculation

Signal processing and spectral analysis methods allow for defining the harmonic frequency components that ferroresonance cause but nonlinear dynamics related to chaos are not determined briefly. The most useful tool for determining chaos is calculating the Lyapunov exponents of the system. Lyapunov exponents are offered by Russian mathematician Alexandr Lyapunov in 1892 in his PhD thesis. This is the first proper definition of stability which is based on the linearization of the equations of the motion [75]. The Lyapunov exponents are useful for defining the evolution of the motion and understanding the stability of the system, whether it is a fixed point, periodic motion, quasi-periodic motion or chaotic motion [76].

The basic idea of Lyapunov exponents is to understand if two very near points on an attractor are converging to each other or diverging from each other through time. Let's consider two points in a space, x_0 and $x_0 + u_0$, each of which will generate an orbit in that space using some equation or system of equations. In Figure 3.4, the separation of these points are given.

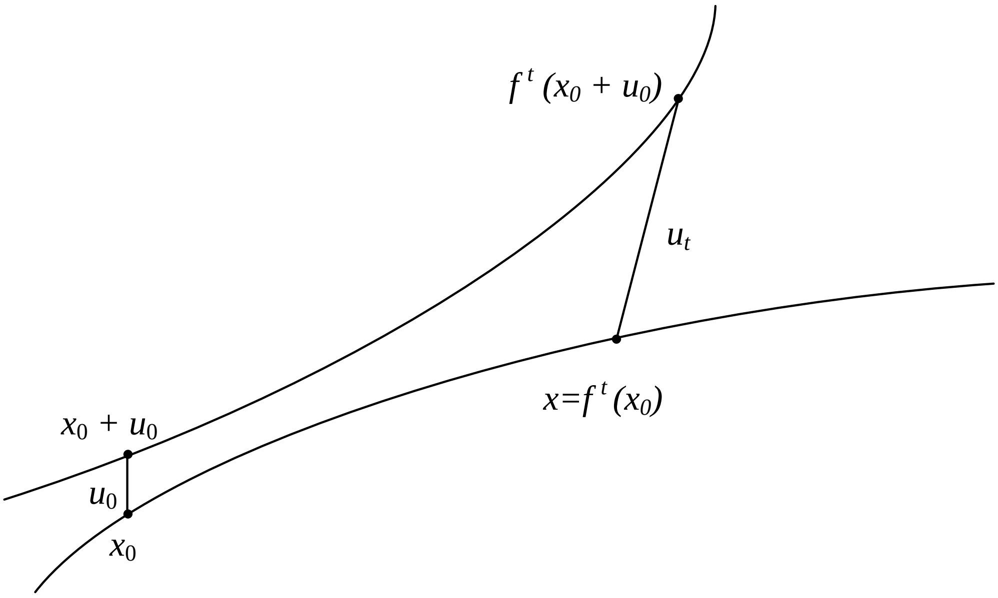

Figure 3.4 : Seperation of nearby points by time.

By calculating the divergence of the orbits, one can define the Lyapunov exponents. A positive exponent stands for the divergence of the orbits which is an indicator for chaotic motion where a negative exponent stands for a periodic motion. If the exponent is calculated as zero, it stands for quasi-periodic motion. If the differential equations of the system are known, the Lyapunov exponents can be calculated analytically.

An n-dimensional autonomous system is given in Equation 3.6.

$$x' = F(x; M) \qquad \textbf{(3.6)}$$

Where;

x: n state variables,

F: Nonlinear evolution of the system,

M: Control parameters

Perturbing the system X(t) by an infinitesimal y(t) and linearizing the system, the perturbation is derived by;

$$\frac{dy(t)}{dt} = Ay(t) \tag{3.7}$$

Here, A is an n x n Jacobian matrix. Considering an initial deviation of y(0), the solution of the system after t times is achieved by;

$$y(\mathrm{t})=\phi(t)y(0) \tag{3.8}$$

Where ϕ(t) is the fundamental matrix solution of the system x(t).

Lyapunov exponents are actually the generalization of eigenvalues of the system. If the system is linearized at a very specific point and the eigenvalues are calculated, these are called local Lyapunov exponents. But in order to talk about the dynamic behaviors of the system, these exponents should be calculated not only at specific points but also for all other points of the system. These are called global Lyapunov exponents. It is clear that, what we are actually looking for is the rate of convergence or divergence of the trajectories. This separation is assumed to be exponential. The calculation of the Lyapunov exponent is given in Equation 3.9.

$$\overline{\lambda_\iota} = \lim_{t\to\infty} \frac{1}{t} \ln \frac{||y(t)||}{||y(0)||} \tag{3.9}$$

Where || || is the vector norm and λ_i is the i^{th} Lyapunov exponent. Since the state is n dimensional, it is clear that the number of Lyapunov exponents will be equal to n. If the exponents are arranged from greatest to smallest, this is called the Lyapunov spectrum, which is given in Equation 3.10.

$$\overline{\lambda_1} \geq \overline{\lambda_2} \geq \cdots \geq \overline{\lambda_n} \tag{3.10}$$

It is not very easy to calculate n Lyapunov exponents with this method, because choosing an initial deviation $y_i(0)$ at random and performing a numerical integration of Equation 3.8 for very large values of *t* causes overflow errors. That would lead to the calculated $y_i(t)$ to align exponentially in the expanding direction. For overcoming this problem, the Gram – Schmidt procedure is proposed. The procedure starts with choosing m orthonormal initial vectors y_i such that y_1=(1, 0, 0, ….), y_2=(0, 1, 0, 0…) and so on, integrating Equations 3.8 and 3. 9 with these initial conditions for an finite time T and finally obtain a new set of vectors $y_1(T)$, $y_2(T)$, …, $y_m(T)$. These new sets of vectors are orthonormalized using the Gram-Schmidt procedure;

$$\hat{y}_1 = \frac{y_1(T)}{||y_1(T)||} \quad \textbf{(3.11)}$$

$$\hat{y}_2 = \frac{y_2(T) - [y_2(T)\hat{y}_1]\hat{y}_1}{||y_2(T) - [y_2(T)\hat{y}_1]\hat{y}_1||} \quad \textbf{(3.12)}$$

$$\hat{y}_m = \frac{y_m(T) - \sum_{i=1}^{m-1}[y_m(T)\hat{y}_i]\hat{y}_i}{||y_m(T) - \sum_{i=1}^{m-1}[y_m(T)\hat{y}_i]\hat{y}_i||} \quad \textbf{(3.13)}$$

where $(\underline{x}\ \underline{y})$ is the scalar product of vectors. Using these vectors as the new initial vectors for integrating the system and carrying out the procedure for a sufficient time, (T_f), the Lyapunov exponents are achieved. The norm in the denominator is named as N_{jk} where k is the kth time step and j is the jth vector. The Lyapunov exponents, λ_i are given in Equation 3.14.

$$\lambda_i = \frac{1}{rT_f}\sum_{k=1}^{r} ln\, N_i^k \quad \textbf{(3.14)}$$

where r is the number of orthonormalizations and T_f is the finite time [77, 78].

4. POWER SYSTEM MODELING

This chapter is related to the power system modeling and equivalent equations of the circuits. For this study, West Anatolian Power System of Turkey is examined and modelled by using the official data of TEIAŞ, TEÜAŞ and TEDAŞ [38]. For ferroresonance studies, a sub-network is chosen from West Anatolian Power System. The sub-network is “Seyitömer-Işıklar line”, which consists of a thermal power plant, a transformer, a 284 km power line and a load.

4.1 Simulink Model

As been previously defined, ferroresonance is an unpredictable phenomenon. It is usually not possible to collect ferroresonance data from a live power system. On the other hand, modeling the system with its real data is a powerful tool. For this study, a MATLAB-Simulink Model is built. In Figure 4.1 the Simulink model is given.

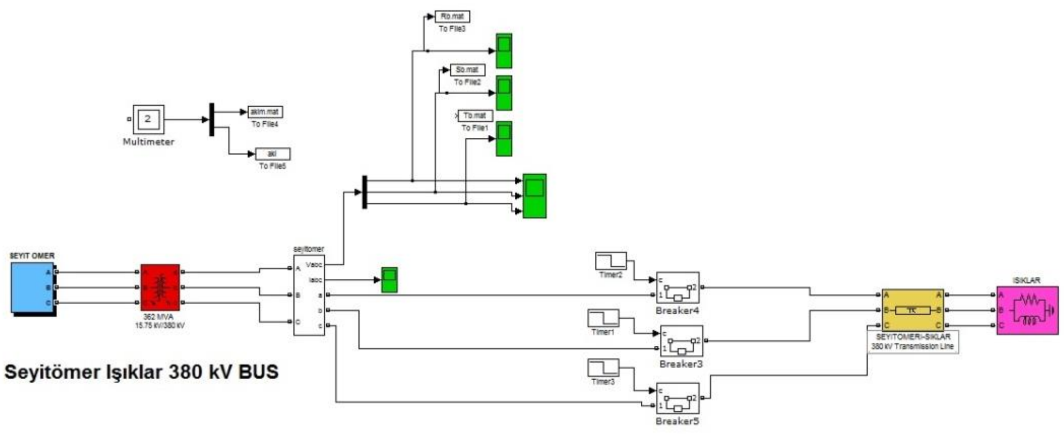

Figure 4.1 : The Simulink model for the Seyitömer-Işıklar line.

In this simulation, the blue block stands for Seyitömer power plant. The red block stands for the the step up transformer. The yellow block is the transmission line between Seyitömer and Işıklar and the pink block stands for Işıklar load. The detailed parameters related to the components are given in Table 4.1. The other blocks are used for data collecting and measurements.

Table 4.1 : System parameters.

Equipment	Parameters
Generators	180 MVA 15.75 kV Rs=2.8544 10^{-3} Ω Ls=5.934 10^{-3} H
Transformer	362 MVA 15.75/380 kV R_{11}=0.0013705 Ω L_{11}=0 H $R_{12'}$=2.3934 Ω $L_{12'}$=0.4571 H R_{fe}=342.63 Ω L_{fe}=1.0906 H
Line	R_1=0.0344 Ω/km R_0=0.292 Ω/km Length=284.341km
Load	361 MWA 6 MVAr

In order to simulate ferroresonance, a 4 second simulation is run. During this simulation, circuit breakers are switched off at the 2nd sec and for simulating the sudden drops of loads. The data collected will be analyzed in Chapter 5.

4.2 Equivalent Circuit of the Power System

The Simulink model is used for simulating ferroresonance and collecting data but this model is not enough for dealing with nonlinear dynamics of ferroresonance. In order to calculate the nonlinear dynamics of ferroresonance, using an analytical approach is a necessity, which brings using a mathematical method as an obligation. For building up this mathematical method, the power system should be modelled by its equivalent circuit.

The equivalent circuit for the whole power system is given in Figure 4.2.

Here;

E_g is electromotive force of the generator,

L_g is the inductance of the generator,

R_g is the resistance of the generator,

R_{11} is the primary winding resistance of the transformer,

L_{11} is the primary winding inductance of the transformer,

R_{12}' is the secondary winding resistance of the transformer

L_{12}' is the secondary winding inductance of the transformer,

r_{fe} is the equivalent core loss resistance,

x_{fe} is the magnetising reactance.

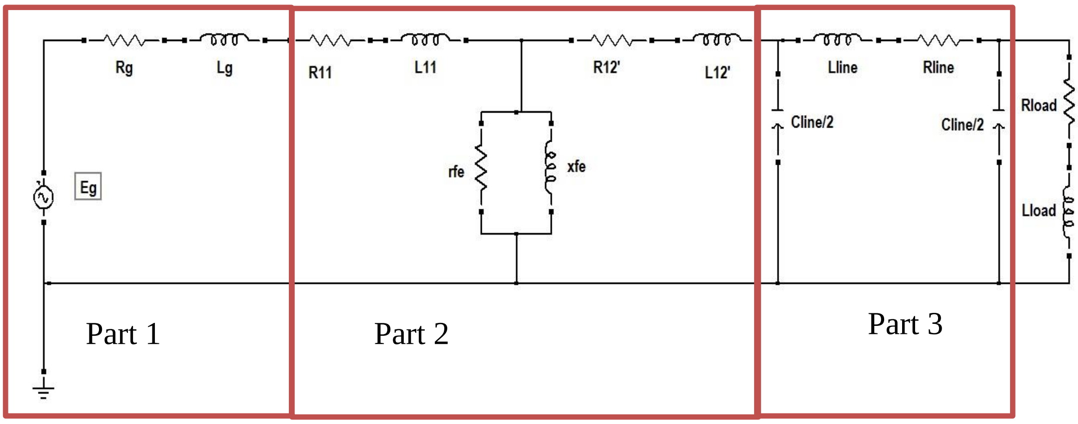

Figure 4.2 : The equivalent circuit of the whole power system.

4.2.1 Equivalent circuit for the transformer

Transformer modeling is the most important point of ferroresonance phenomena as the nonlinear iron core is the main cause of occurrence of the ferroresonance. It was stated in Chapter 1 that, the losses should not be neglected for a proper modeling. Using the Tee-equivalent circuit of the transformer allows for modeling the transformer with its losses and this model is the most accurate equivalent circuit. The series resistance stands for copper losses. Iron losses are divided into two as Eddy currents and hysteresis losses and they are simulated by R_{fe} [79]. Although, magnetic coupling between the phases of transformer should be considered, it was previously stated that for one phase transformers, coupling can be neglected. In spite of the fact that, the transformer is 3 phase, the coupling is neglected because the simulations and calculations for nonlinear dynamics are performed for one-phase [12, 80]. In Figure 4.2, Part 2 is the Tee-equivalent circuit of the transformer.

4.2.2 Equivalent circuit for the power line

Transmission lines are modelled according to their length. As the length of the transmission line increases, the model should involve all the parameters that affect the performance of the line. Line capacitances can be neglected for short transmission lines, which are shorter than 80 km. On the other hand, as the length of the transmission lines increase, the effect of line conductance is added. For medium length, i.e. length is between 80 km and 250 km, a π equivalent transmission line model is used. If the transmission line is long, i.e. longer than 250 km, the lumped parameter π circuit is not sufficient for modeling and the distributed parameter π circuit is used. The equivalent circuit is given in Figure 4.3 [1, 81].

The series impedance per length is given by Equation 4.1 and shunt capacitance is given by Equation 4.2

$$z = r + jwl \tag{4.1}$$

$$y = g + jwc \tag{4.2}$$

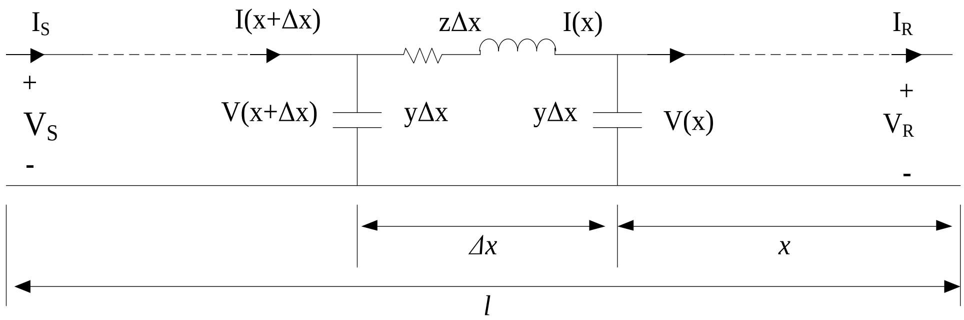

Figure 4.3 : The distributed parameter π - equivalent circuit model for long lines.

In Figure 4.4 the equivalent π circuit for long line model is given.

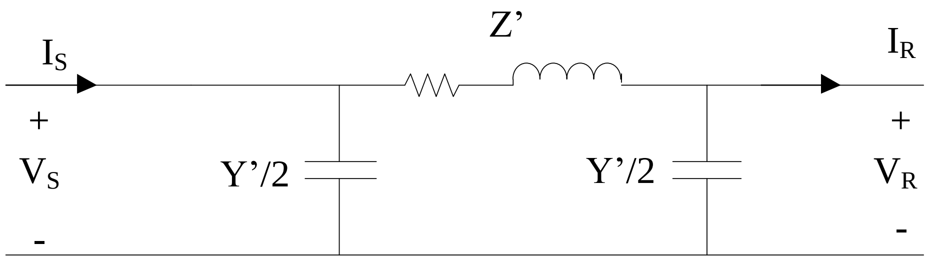

Figure 4.4 : The equivalent π circuit for long line model.

Parameters of the equivalent π – line are given in Equations 4.3 and 4.4 respectively.

$$Z' = Z\,\frac{\sinh(\gamma l)}{\gamma l} \tag{4.3.}$$

$$\frac{Y'}{2} = \frac{Y}{2}\,\frac{tanh\,(\frac{\gamma l}{2})}{\frac{\gamma l}{2}} \tag{4.4}$$

Where;

$\gamma = \sqrt{z\,y}$: propagation constant

l : length of the power line

4.2.3 The equivalent circuit for generators

A simple equivalent model consisting of a sinusoidal voltage source, a resistance and an inductance is used. Since a sinusoidal voltage source is sufficient for occurrence of ferroresonance, more complicated two axis generator models are not utilized. In Figure 4.2 part 1 stands for the equivalent circuit of generators.

5. DATA PROCESSING AND SPECTRAL METHODS

Ferroresonance is an irregular process and thus it is usually difficult to identify. In order to force the power system to operate under ferroresonance conditions, the circuit breakers are opened at 2^{nd} second. A total of 4 seconds. of simulation is run and the voltage and current variations for the three phases are collected. In Figure 5.1 the voltage variations are given. As the three phases are identical, for further calculations the voltage variations for phase R are used. The detailed voltage variation for phase R is given in Figure 5.2.

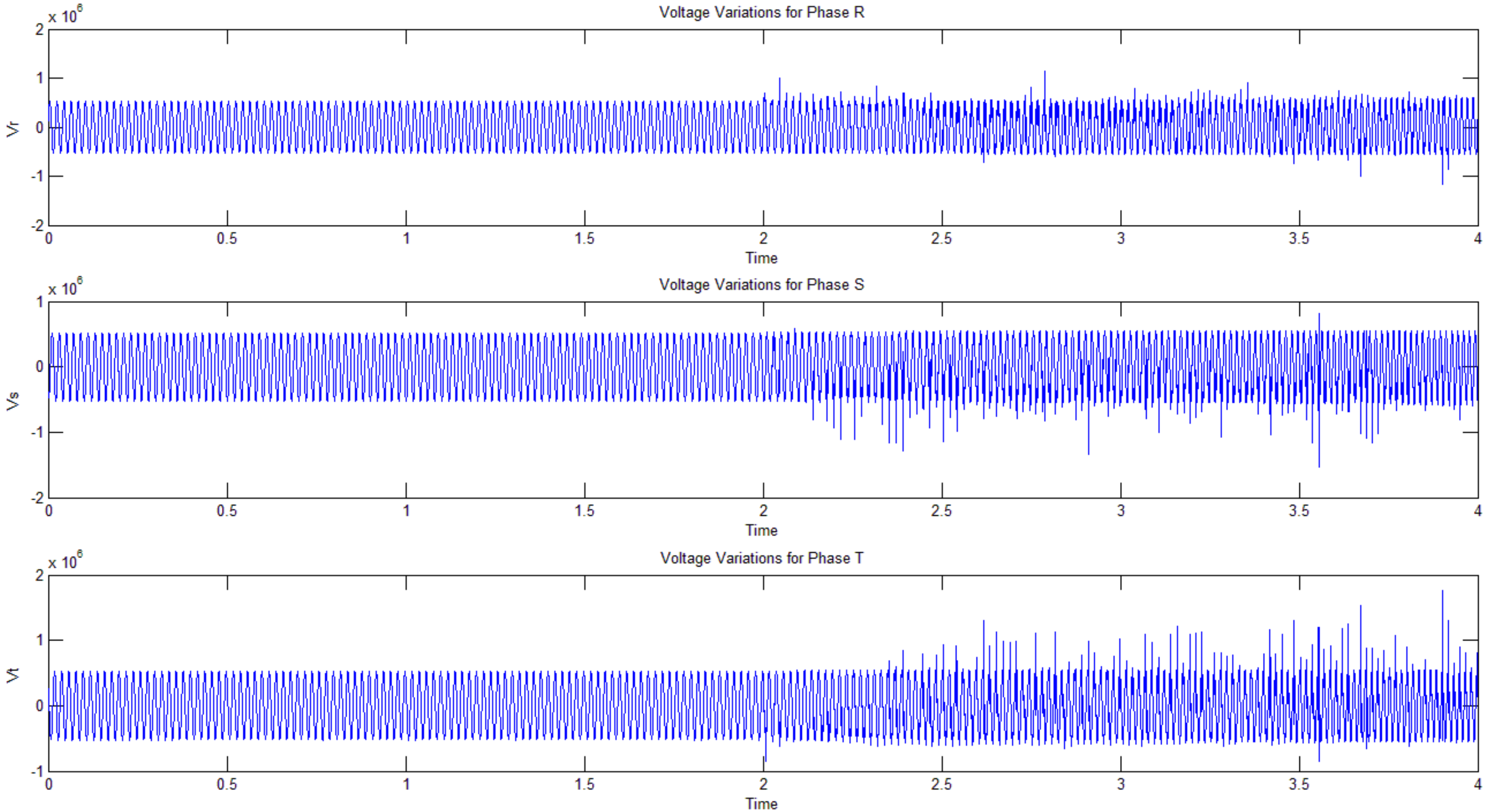

Figure 5.1 : The voltage variations for R-S-T phases.

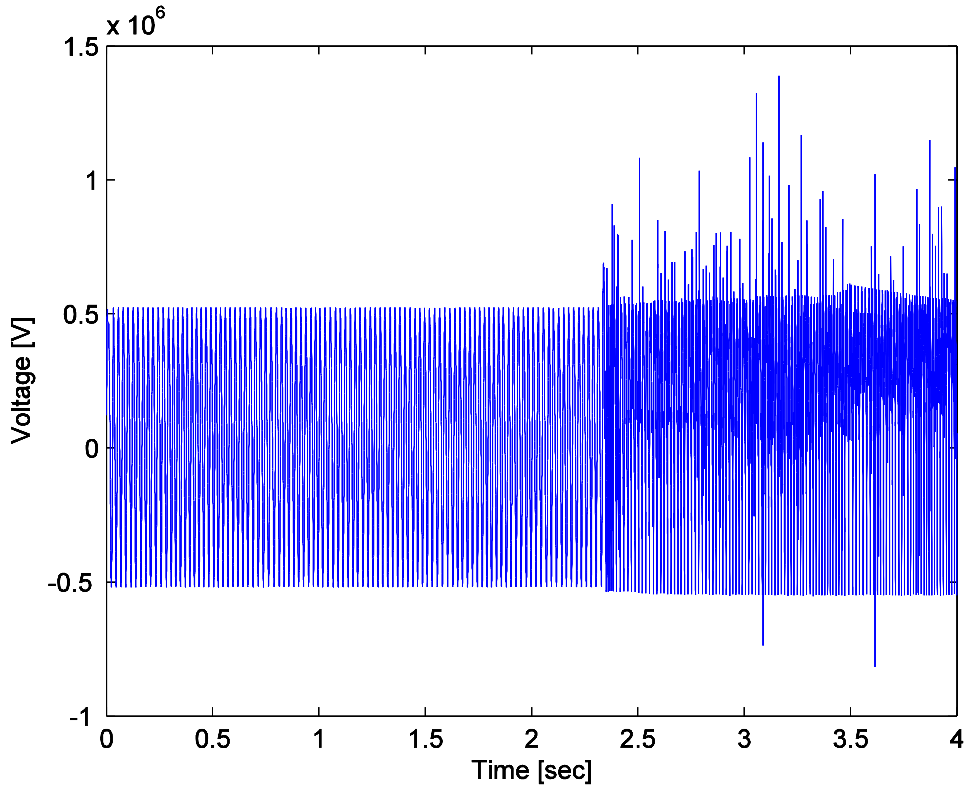

Figure 5.2 : The voltage variation for phase R.

The effect of the ferroresonance can be observed after the 2nd second.

5.1 Spectral Data Analysis

The ferroresonance data considered in Figure 5.1 and Figure 5.2 are nonstationary thus the total data are split into two parts, namely pre-ferroresonance and post-ferroresonance. By this way, two stationary data sets are achieved. The short tTime Fourier transform (STFT) of the total signal for phase R is given in Figure 5.3.

The fundamental frequency of the system, which is 50 Hz, is observed through out the whole signal duration. On the other hand, it is also clear that there are high frequency components with huge amplitudes lying in the post - ferroresonance region. It is an indication that ferroresonance generates high frequency components. In power system harmonic studies, the frequency components higher than the 10^{th} harmonic are usually omitted. For frequency components above approximately 500 Hz, the amplitudes tend to be smaller. Thus 500 Hz is chosen as a threshold value for further investigations.

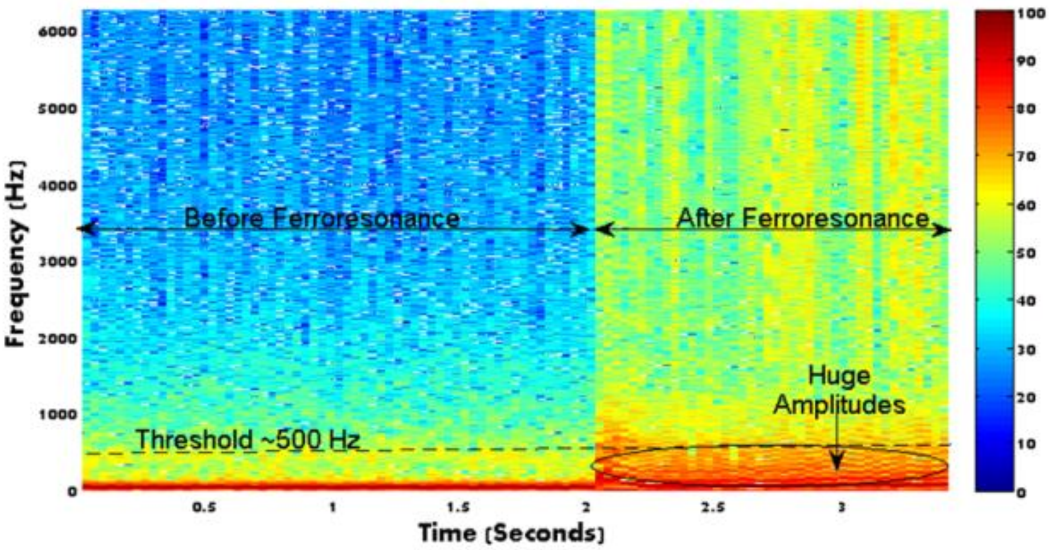

Figure 5.3 : The STFT for voltage variations of phase R.

Although STFT gives a general opinion about the occurrence of high frequency components, the values of exact frequencies and which steady state mode is caused by ferroresonance are still not clear. In order to overcome this problem, multi resolution wavelet analysis (MRWA) is applied. The first concern about MRWA is to decide the number of decompositions for the signal. The signal should be decomposed properly without gaps or overlapping, so that the process is always reversible. A decision criterion is settled according to Equation 5.1.

$$N = log_2(Fs/Fw) \qquad \textbf{(5.1)}$$

Where;

N= Level of decomposition (sub-bands)

Fs=Sampling frequency

Fw=Desired frequency to be observed

The sampling frequency is 12500 and the desired frequency is 500 Hz. N = 4.64. N can be rounded up or down. For this study, N is chosen as 4. By 4 level of decomposition, 0 - 390 Hz frequency band stands for the 4th approximation. In Table 5.1, frequency ranges of the related sub–bands are given.

Table 5.1 : Frequency intervals of related sub–bands.

Sub – bands	Frequency ranges (Hz)
d_1	3125 – 6250
d_2	1562 – 3125
d_3	781 – 1562
d_4	390 – 781
a_4	0 - 390

The second concern is choosing the right mother wavelet. As a rule of thumb, the shape of the mother wavelet should be similar to the shape of the original signal to be decomposed. In our case, Daubechies mother wavelet family is suitable with their orthonormal characterization.

After deciding on the level of decomposition and choosing the proper mother wavelet, the MRWA is applied and signal is decomposed. In Figure 5.4 the 4th approximation for the pre -ferroresonance region is given. It is clearly seen that, the system has a fundamental frequency of 50 Hz. On the other side, the frequency component at 100 Hz with a small amplitude is also observed. As has been previously stated, chaotic behaviors are dependent on initial conditions. The 2nd harmonic in power systems stands for an unbalanced operation. It can be said that, despite operating under normal conditions, this system has abnormalities too.

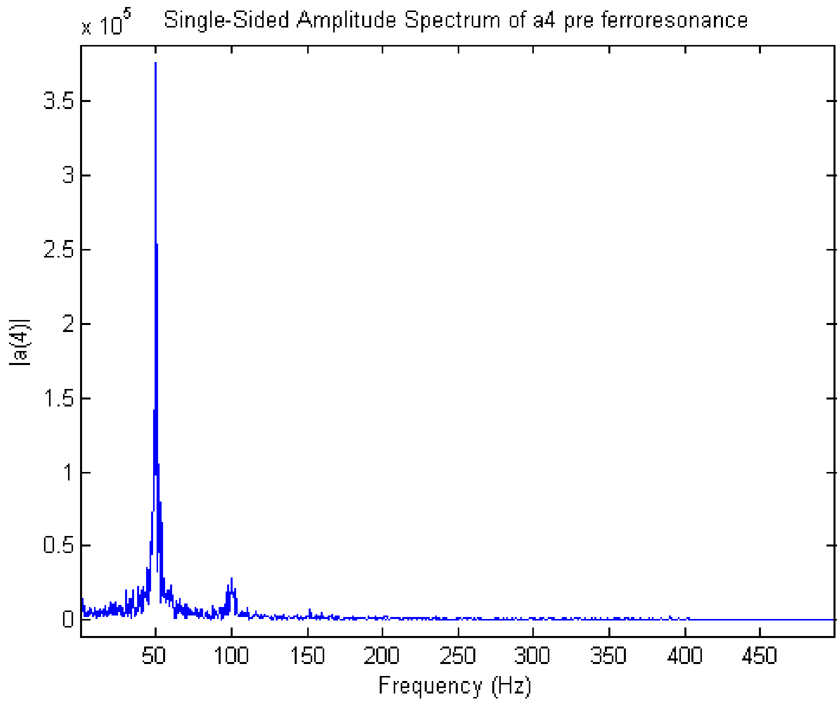

Figure 5.4 : The 4th approximations for pre - ferroresonance region.

In Figure 5.5, the 4th approximation for the post - ferroresonance region is given. It is clearly seen that there are many harmonic frequency components in addition to the fundamental frequency and the 2nd harmonic.

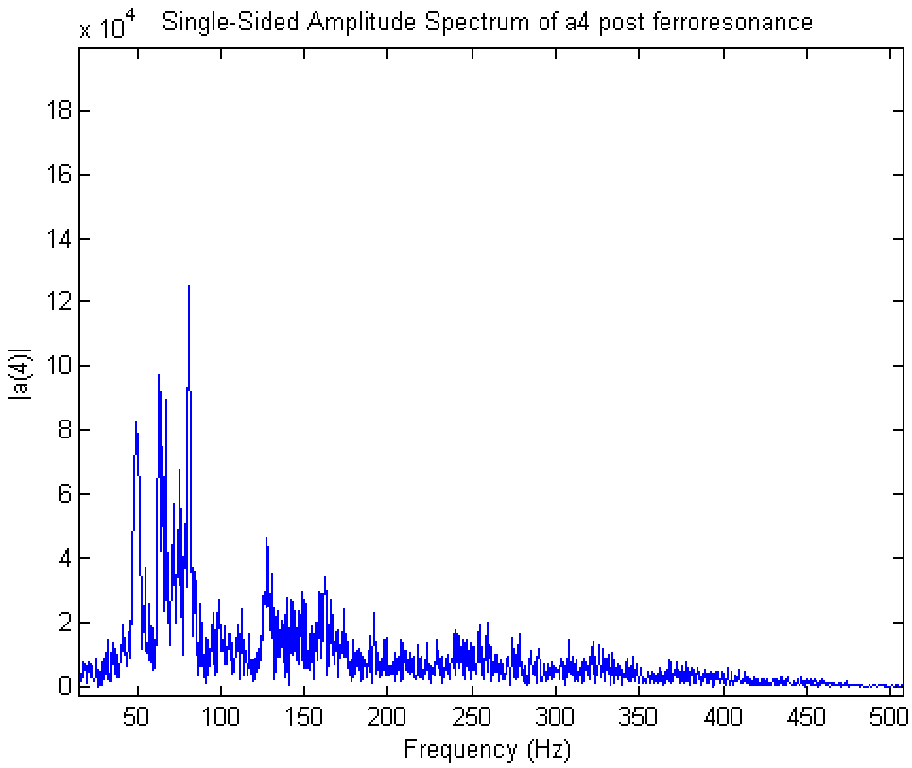

Figure 5.5 : The 4th approximations for post - ferroresonance region.

Although approximations give brief information about the harmonic frequency components, it is also a wise idea to control the details and examine the change of high frequency components. In Figure 5.6 the details for the pre - ferroresonance region are given. Although, the system was operating in a perfectly stable condition, there are still high frequency components with small magnitudes.

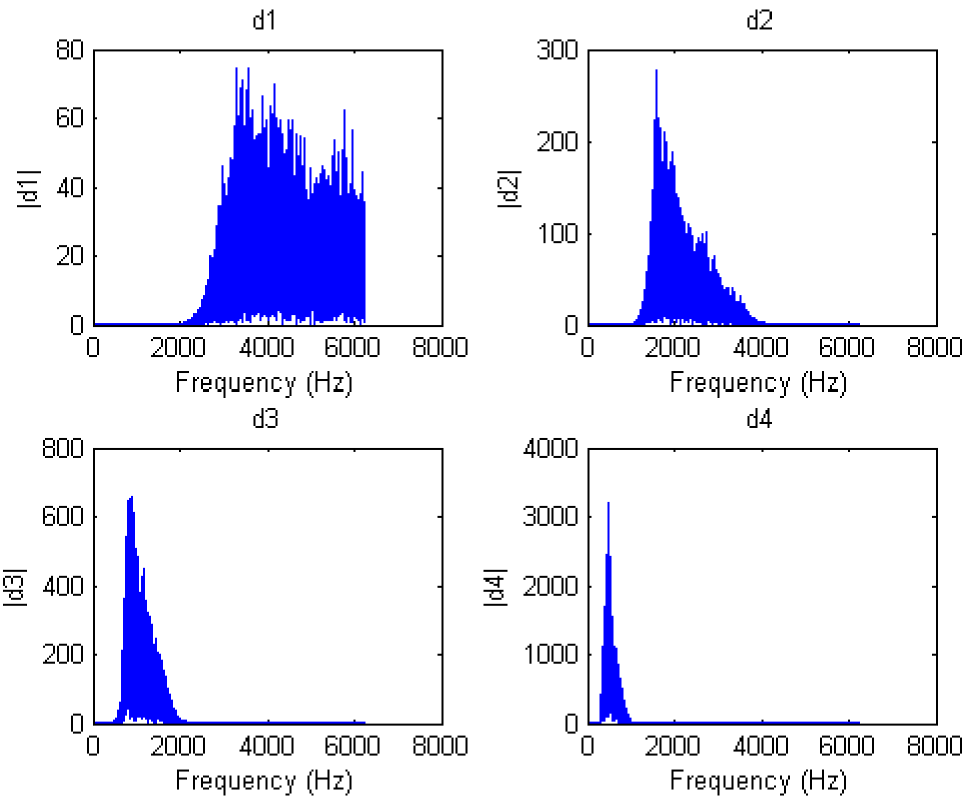

Figure 5.6 : The details for pre – ferroresonance region.

In Figure 5.7 the details for the post – ferroresonance region are given. Comparing the amplitudes of high frequency components with the pre – ferroresonance region, it is observed that the amplitudes got higher. Ferroresonance did not only cause harmonic components on the low frequency band, but also caused amplification of amplitudes on the high frequency band. The details also prove that, ferroresonance is dependent on its initial conditions. Although 50 Hz was expected to be the only fundamental frequency in the pre – ferroresonace region, MRWA points out that the system also has other high frequency components with small amplitudes. From this indication, further studies are carried out to find out if the system is running in a chaotic mode.

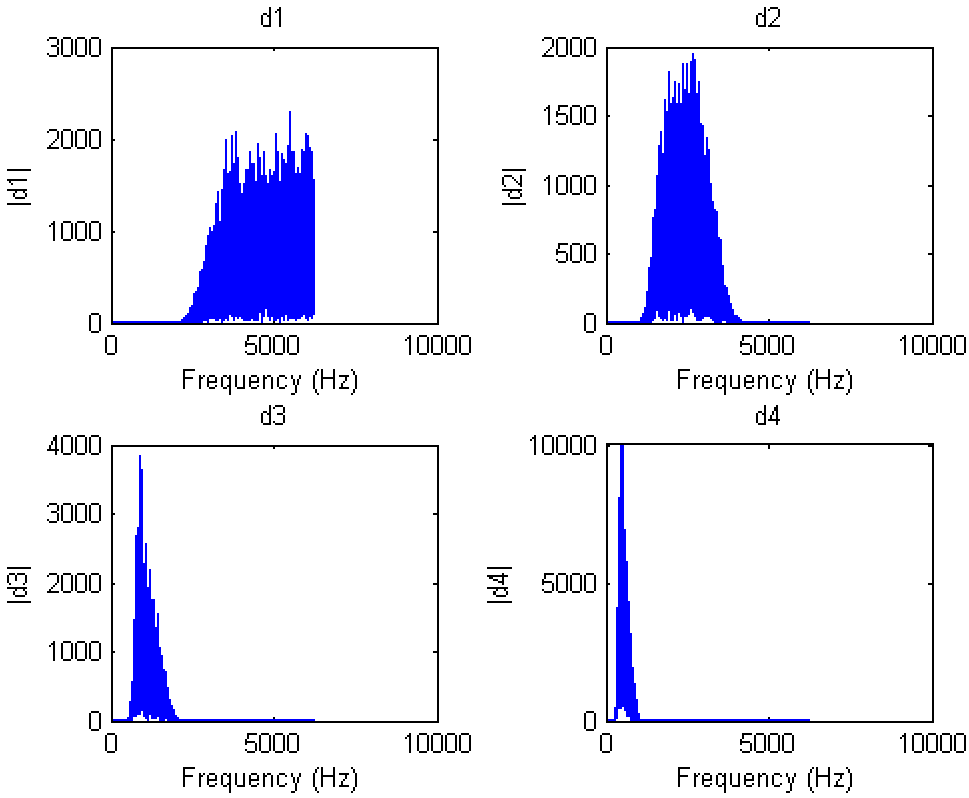

Figure 5.7 : The details for post – ferroresonance region.

5.2 Determining Frequency Components and Related Interpretation

In the previous section, the related frequency components to ferroresonance were examined. Although, it is clear that ferroresonance is responsible for these components, in order to determine the steady state behaviour of the system, the approximation for post – ferroresonance region is examined briefly.

In Figure 5.8 the sub harmonic band for post – ferroresonance region is given. Frequency components of 10 Hz, 12.5 Hz and 25 Hz are observed which are 1/5, ¼ and ½ times of the fundamental frequency, 50 Hz. The ferroresonance caused sub harmonic frequency components.

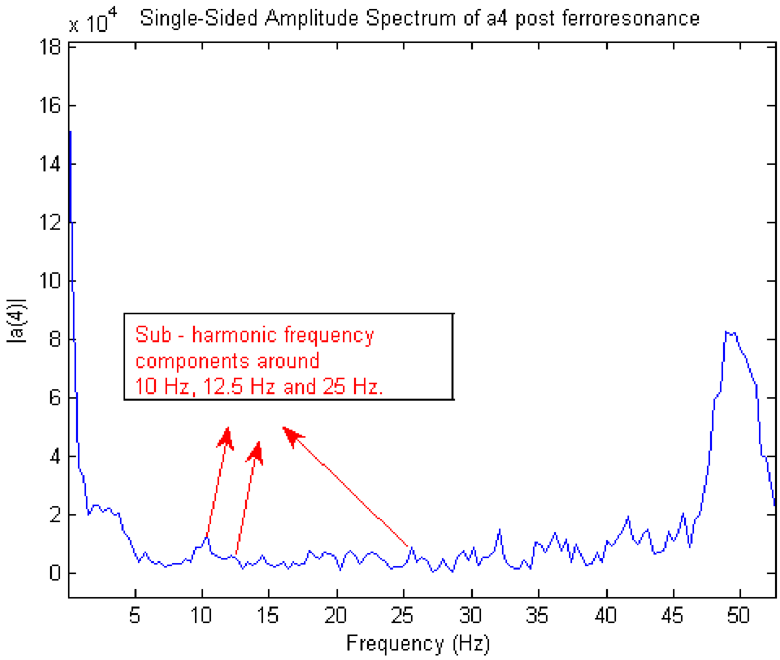

Figure 5.8 : The sub harmonic frequency band for post – ferroresonance region.

In Figure 5.9 the frequency band between 50 Hz and 200 Hz is given. In this frequency band, several peaks are observed.

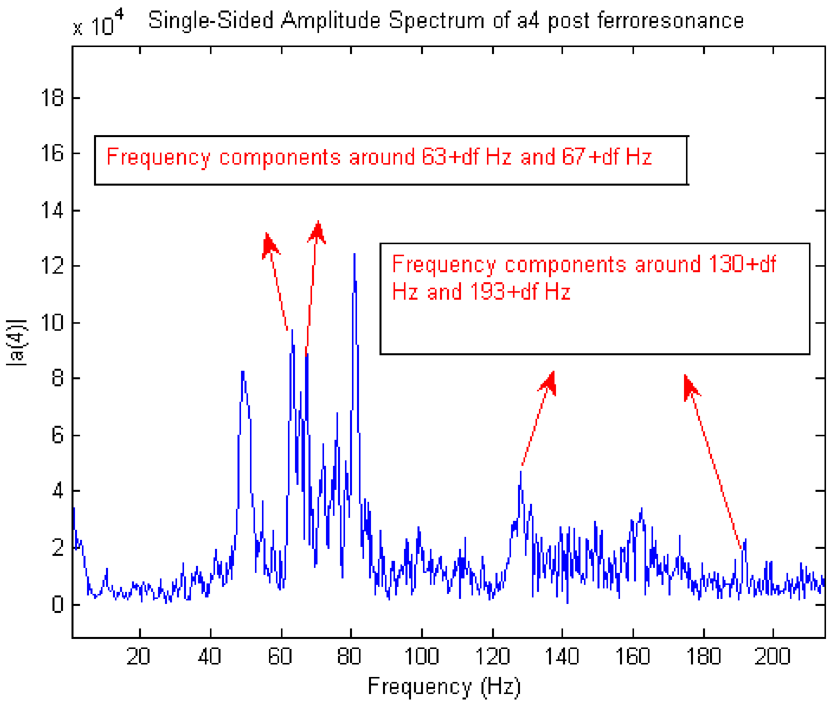

Figure 5.9 : The quasi periodic frequency band for post – ferroresonance region.

It was previously stated that, if a new frequency component with nf_1+mf_2 can be achieved then these components are called quasi periodic frequency components. In the post - ferroresonance region, the frequency components between 50 Hz and

100± Δf Hz and also 130±Δf Hz and 193 ± Δf Hz are observed. For f_1=63 ± Δf Hz and f_2 = 67 ± Δf Hz, frequency at 130 ± Δf Hz is achieved with respect to n = 1 and m = 1. For n = 2 and m = 1, a frequency at 193 ± Δf Hz is achieved. 63 ± Δf Hz and 67 ± Δf Hz are detected in the frequency band spectrum as well as 130 ± Δf Hz and 193 ± Δf Hz.

The phase portrait of the quasi periodic waveforms is a two dimensional torus and the Poincaré map forms a closed loop [82, 83]. In Figure 5.10, the phase portrait for the entire signal is given. It is clear that, for the pre – ferroresonance region, the phase portrait only shows the periodic motion. For the post – ferroresonance region, it is not easy to identify the motion because the current suddenly drops to zero. For a better explanation the phase portraits are plotted separately and given in Figure 5.11.

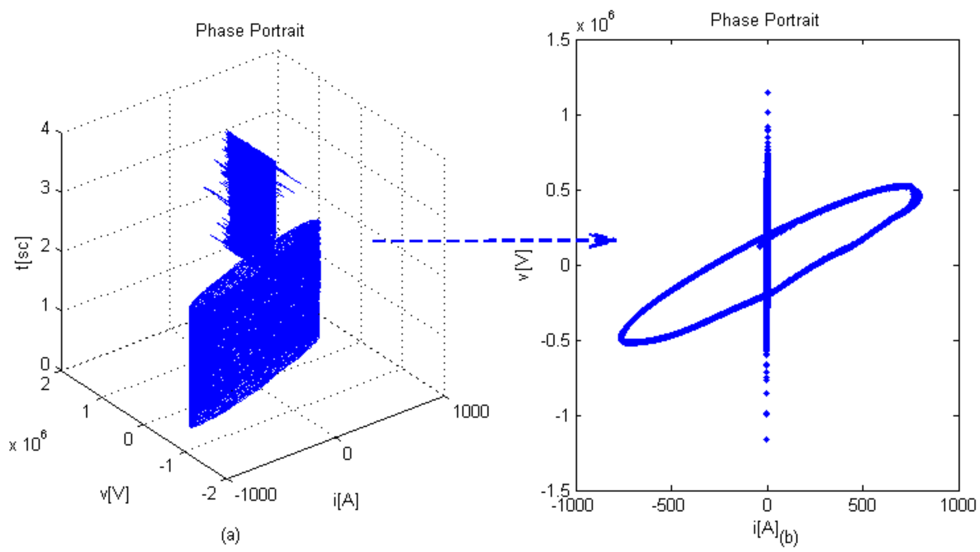

Figure 5.10 : Phase portraits for the entire signal (a) 3D. (b) 2D.

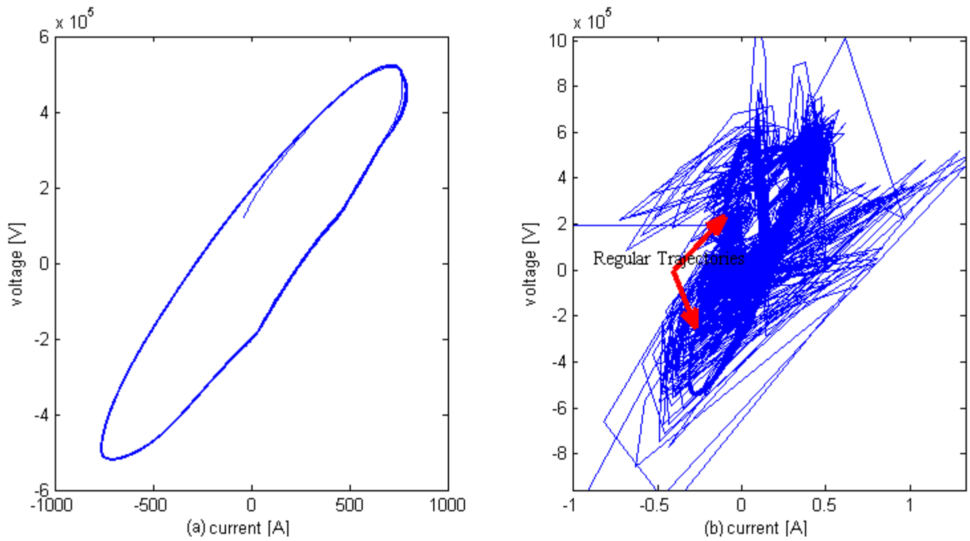

Figure 5.11 : Phase portraits for (a) Pre – ferroresonance. (b) At the beginning of ferroresonance.

According to the phase portraits, the effects of ferroresonance cannot be seen in the pre-ferroresoance region, meaning the system is oscillating only with the fundamental frequency of the system which is 50 Hz. Besides the post-ferroresonance region, there are regular trajectories and other frequency components and some noise. Using the wavelet transform, it is proved that there are quasi-periodic and sub harmonic frequency components in the system. The previously mentioned trajectories stand for these harmonic components [84]. Nevertheless, constructing a mathematical equation for the RLC circuit and proving the steady state response of ferroresonance will be a convenient way.

6. NONLINEAR DYNAMICS OF THE EXPERIMENTAL DATA

The Lyapunov exponent is a very important indicator of chaotic behavior. A Lyapunov exponent greater than zero usually implies a deterministic chaos [75] but it is not the only indicator so further calculations should be done such as recurrence plots. A system with a Lyapunov exponent greater than zero, and a periodical recurrence plot, is not classified as chaotic, but it is classified as sensitive to the initial conditions.

This chapter will focus on attractor reconstruction, Lyapunov exponent calculation and obtaining the recurrence plots of the examined ferroresonance data. Through these methods, it will be possible to classify the nonlinear dynamics of the experimental data.

6.1 Attractor Reconstruction

Analytical calculation of Lyapunov exponents is not a straightforward process even with the systems which do not have excessive dimensions. On the other hand, it is not always possible to know the differential equations of the system. Especially, experimental data sets might have high order differential equations. Modeling the system with differential equations is not a simple process. For overcoming this issue, several approximations are proposed for determining the Lyapunov exponents from time series.

The first step is constructing the phase space of the system. The phase space is assemblage of possible states of the system. It means that, if all information of the system at any time instance *"t"* is known, it is possible to forecast the future system states. If the system is mathematically known the phase space is easily constructed from the equations of motion. If the system is not known, then the phase space should be reconstructed from the time series. Reconstructing the phase space is explained by Whitney and Takens embedding theorem [85]. According to Whitney's embedding theorem, an n dimensional manifold is an embedding to a 2n+1 dimensional Euclidean space. The embedding has the same properties, for example

Lyapunov exponents, with the original system. The main problem is to determine the embedding dimension briefly so that the manifold should be unfolded correctly, i.e. any two points of the manifold should not correspond to the same points in the 2n+1 dimensional space. Takens contribution to this theory is that, the embedding dimensions can be computed directly from a single measured quantity. According to Takens, instead of having 2n+1 generic signals, the time delayed vectors $[y(t),y(t-\tau),y(t-2\tau),\ldots,y(t-2n\tau)]$ of one generic signal would be sufficient to embed the n - dimensional manifold [85, 86].

6.1.1 Determining time delay

For a successful reconstruction of the phase space, time delay τ should be chosen. There are two main methods to choose τ. First one is examining the mutual information of the time series and second one is calculating the zero passing point of autocorrelation function.

Mutual information is used for understanding the relationship between two discrete variables. If mutual information is calculated as zero, these variables are independent from each other. The mutual information of two variables is given in Equation 6.1.

$$\mathrm{I}(x,y) = \sum_{x,y} P_{xy}(x,y)\, log \frac{P_{xy}(x,y)}{P_x(x)P_y(y)} \tag{6.1}$$

Where, $P_{xy}(x,y)$ is the joint probability distribution function of x and y,

$P_x(x)$ and $P_y(y)$ are the marginal probability distribution functions [87–89].

The autocorrelation function is used to find the cross-correlation of a signal with itself. It is the analogy of the signal with time delay. As Takens embedding theorem proposes to use the signal and its time-delayed versions, autocorrelation function is a very useful tool for determining the amount of time delay [90]. The autocorrelation function is given in Equation 6.2 and 6.3.

$$C_L(T) = \frac{\frac{1}{N}\sum_{n=1}^{N}[x(n+T)-\bar{x}][x(n)-\bar{x}]}{\frac{1}{N}\sum_{n=1}^{N}[x(n)-\bar{x}]^2} \tag{6.2}$$

$$\bar{x} = \frac{1}{N}\sum_{n=1}^{N} x(n) \tag{6.3}$$

In order to find the time delay, the first time that $C_L(T)$ curve passes through the zero should be determined. This allows for understanding the linear dependence of x(n) and x(n+T). But for a nonlinear system, mutual information should be used instead of the autocorrelation function [89, 91, 92].

A MATLAB OpenTSTOOL is used for calculating the mutual information of pre-ferroresonance data [93]. The mutual information graph is given in Figure 6.1 The first minimum point of the mutual information points out the sufficient time delay. It is seen that, 12 is the first minimum point therefore the time delay (τ) is chosen as 12.

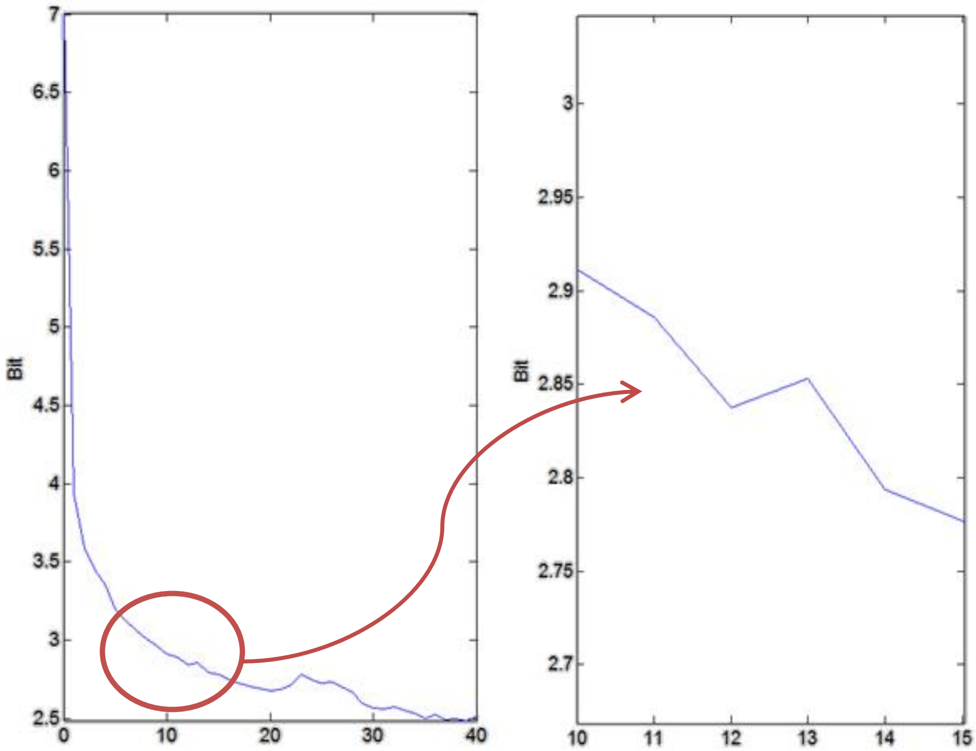

(a) (b)

Figure 6.1 : The mutual information graph for (a) Pre- ferroresonance data. (b) Focused around first minimum.

6.1.2 Determining embedding dimensions

The main idea for Takens embedding theorem is to unfold the attractor of a time series. After determining the time delay, it is crucial to determine the embedding dimensions. The most widely used method for this is the false nearest neighbourhood method. Assume a time series of x(n);

$x(n)= [x(1), x(2), \ldots, x(N)]$

The reconstructed vectors in a d-dimensional space are constituted as;

$Y(n) =[x(n), x(n+\tau),\dots,x(n+(d-1)\tau)]$

Where τ stands for time delay and d is the embedding dimension. It is crucial to find if the time series are unfolded completely therefore the false nearest neighbours are calculated. First, the nearest neighbours of all points in a d-dimensional space are calculated and then the same points for (d+1)-dimensional space are calculated. The Euclidean distance between these points are computed and compared to a threshold value (R_T). This is given in Equation 6.4 [94 – 96].

$$\frac{|y_i^{d+1} - y_j^{d+1}|}{|y_i^d - y_j^d|} > R_T \qquad \textbf{(6.4)}$$

If the calculated value is greater than the threshold value, this shows that the time series is completely unfolded. If not, the chosen d-dimension is not sufficient to unfold the attractor, and a greater dimension should be chosen. The main problem with the false nearest neighbour method is that, there is no good criteria for determining the R_T value. R_T is usually chosen as 15.

For overcoming this issue, Cao's method for embedding dimensions is proposed [97]. This method does not require a threshold value but still, the Euclidean distance between the nearest neighbours are calculated according to Equation 6.5.

$$a(i,d) = \frac{|y_i^{d+1} - y_j^{d+1}|}{|y_i^d - y_j^d|} \qquad \textbf{(6.5)}$$

Different time series might have different threshold values so it might be impossible to detect the proper threshold value. Cao proposes to use the average of *a(i,d)* values to overcome this problem which is given in Equation 6.6.

$$E_d = \frac{1}{N - d\tau} \sum_{i=1}^{N-d\tau} a(i,d) \qquad \textbf{(6.6)}$$

To determine E_d's evolution from d-dimensions to d+1 dimensions,

$$E_1(d) = \frac{E(d+1)}{E(d)} \qquad \textbf{(6.7)}$$

When $E_1(d)$ stops changing, for the values of d greater than a d_0 the time series are said to form an attractor. Also, for separating the deterministic data from stochastic data, a new quantity E_2 is defined which is given in Equation 6.9.

$$E'_d = \frac{1}{N - d\tau} \sum_{i=1}^{N-d\tau} | \, x_i + d\tau - x_{n(i,d)} + d\tau \qquad \textbf{(6.8)}$$

$$E_2(d) = \frac{E'(d+1)}{E'(d)} \qquad \textbf{(6.9)}$$

For a random data, the future values are independent of the past values, so *E₂(d)* will be equal to zero. But for deterministic data, $E_2(d)$ will be changing according to the value of d.

Several trials show that, although Cao's method has advantages over the FNN method, it is a very time consuming process. As the complexity of the system increases, the need for more powerful computers increases too. In addition to this the FNN method responds faster. The size of the data affects the speed of the simulation as well. In Figure 6.2 and in Figure 6.3, the minimum embedding dimension calculated with the FNN algorithm is given [98]. The appropriate value is the point where the percentage of the false nearest neighbours drops down to zero. In the pre-ferroresonance case, the minimum embedding dimension is calculated as 6.

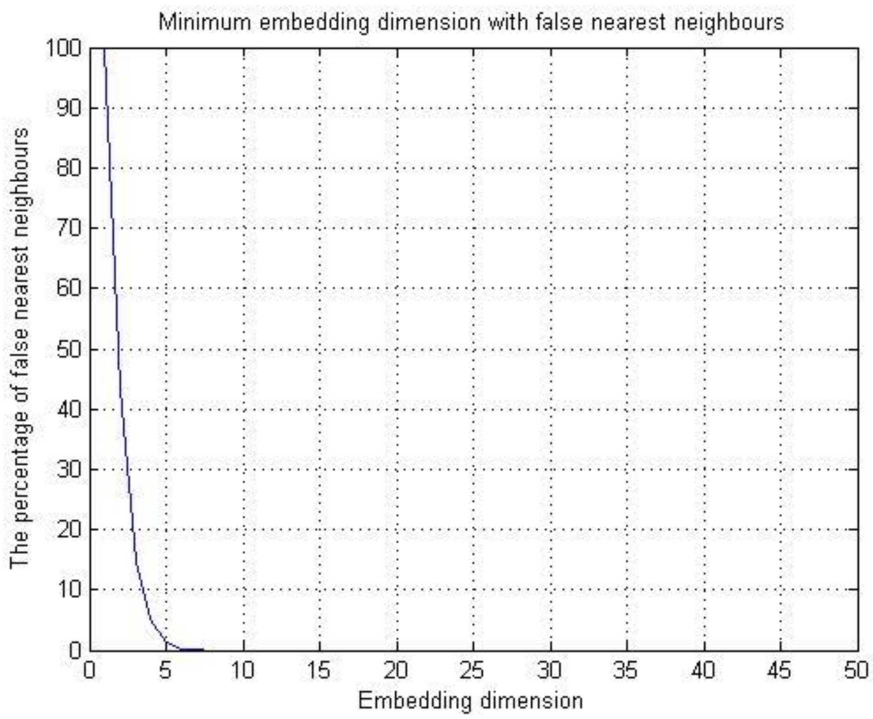

Figure 6.2 : The minimum embedding dimension graph for pre- ferroresonance.

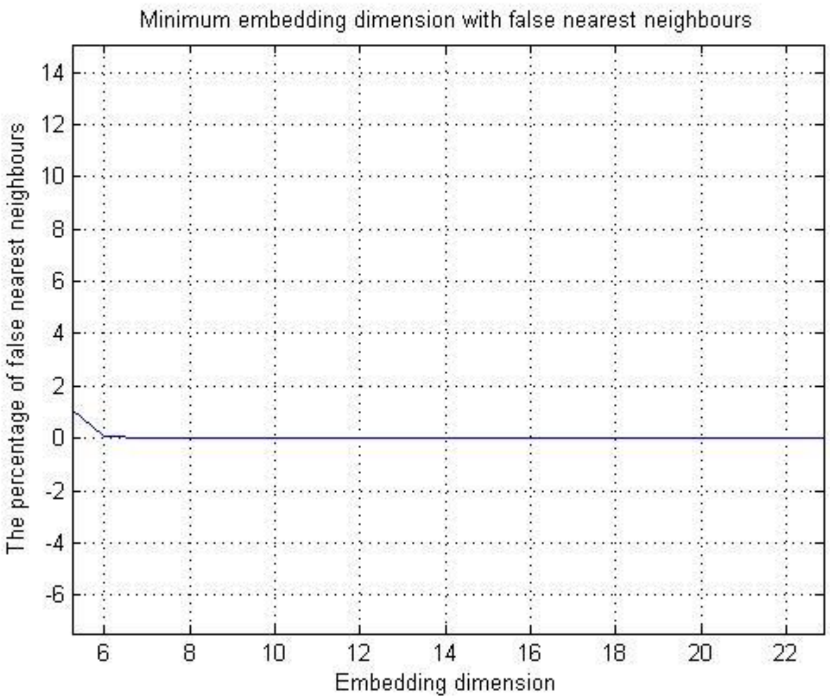

Figure 6.3 : The minimum embedding dimension graph of the appropriate value.

6.2 Largest Lyapunov Exponent

If the exact differential equations of the system are known, the Lyapunov exponents can be calculated. The details for the calculation were given in Chapter 3. On the other hand, it is usually very hard to derive the exact differential equations of real-world problems, so an estimation method depending on the time series should be utilized.

The first study was focused on the evolution of the small perturbations along a long time period in an attractor [77]. Nevertheless, this algorithm is still depending on the differential equations of the system. Since then, research were focused on estimation of the Lyapunov exponents from time series. One of these studies focuses on attractor reconstruction [99]. Once the attractor is reconstructed, the evolutions of two nearby points on a trajectory are examined and the divergence of these points is plotted. A line using the least squares estimation is fitted. The slope of the line is calculated as the largest Lyapunov exponent of the system. Later on, researchers focused on developing better regression algorithms [100, 101].

On the other hand, neural networks are widely used for Lyapunov exponent estimation. The main idea is to estimate the Jacobian matrices and achieving the eigenvalues of the Jacobians. The eigenvalues are related with the local Lyapunov exponents. The first use of this technique was seen in economics [102]. Early papers were using a multilayer feed forward neural networks but later on, different types of neural networks were also used [103 – 105].

For determining the largest Lyapunov exponent of the ferroresonance data, a regression estimation is utilized [106]. It is an easy implementation and a fast responding method. After reconstructing the attractor, two nearby point on a trajectory are chosen and their separation by the Euclidean distance is observed during a finite time period. By recording the divergence of these points, a line is fitted with the least squares method. The divergence is believed to have vertical and horizontal parts. The slope of the line at the vertical part gives the largest Lyapunov exponent of the system.

After reconstructing the attractor for the ferroresonance data with τ=12 and m=6, the divergence of the nearby points is calculated [107]. In Figure 6.4, the divergence of nearby points are given.

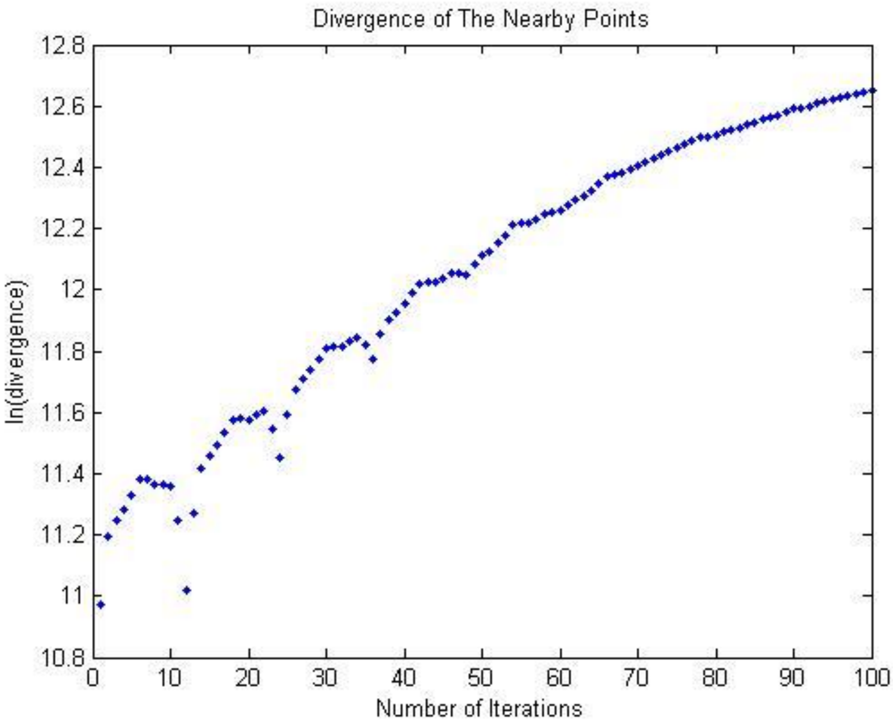

Figure 6.4 : Divergence of nearby points for pre-ferroresonance data.

A first order line is fitted to the divergence points which is given in Figure 6.5. The equation of the fitted data is given in Equation 6.10.

$$f(x)= 0.01562x + 11.26 \quad \textbf{(6.10)}$$

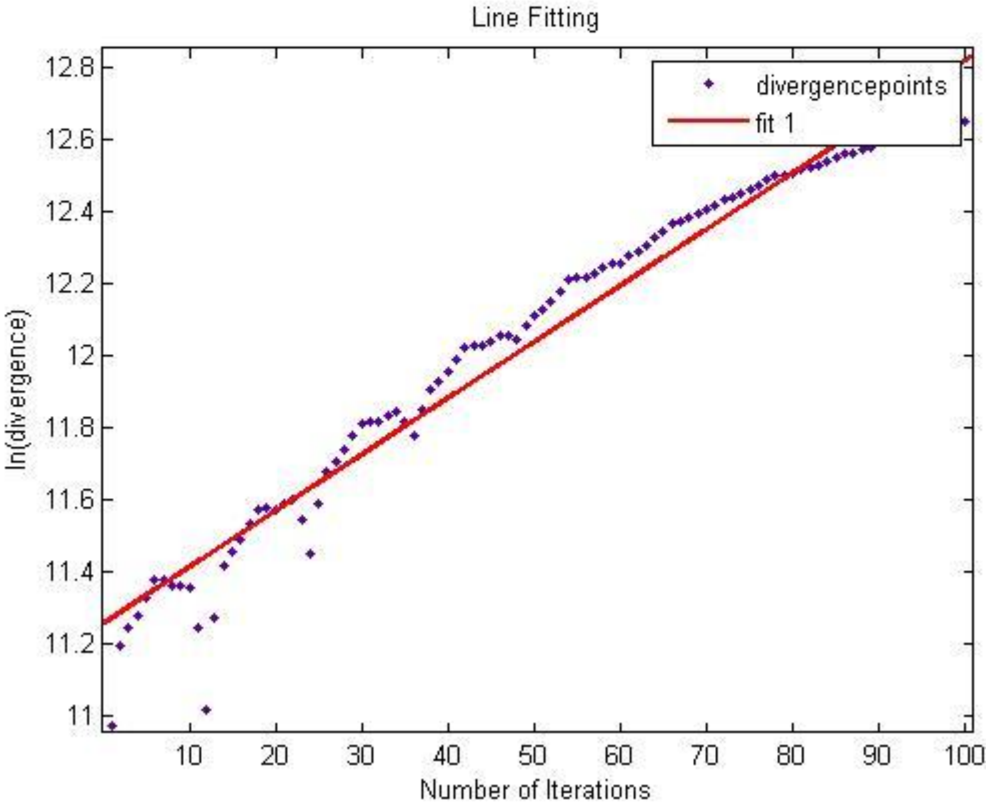

Figure 6.5 : The line fitting to the divergence points.

The slope of the line is 0.01562, which is also the largest Lyapunov exponent (LLE) of the system. The LLE is found to be greater than zero, which is an indication of the chaotic behaviour. On the other hand, it is known that the system has a periodic movement. To be sure, the recurrence plot is constructed with the MATLAB Cross Recurrence Plot (CRP) Toolbox [108].

In Figure 6.6, the CRP of the pre-ferroresonance data is given. It is clear that the recurrence plot is periodic. The system is not in a chaotic mode but it is sensitive to the change of initial conditions. Also, the LLE was computed to be very small; thus the comments related to the chaotic behavior of a system should be done carefully.

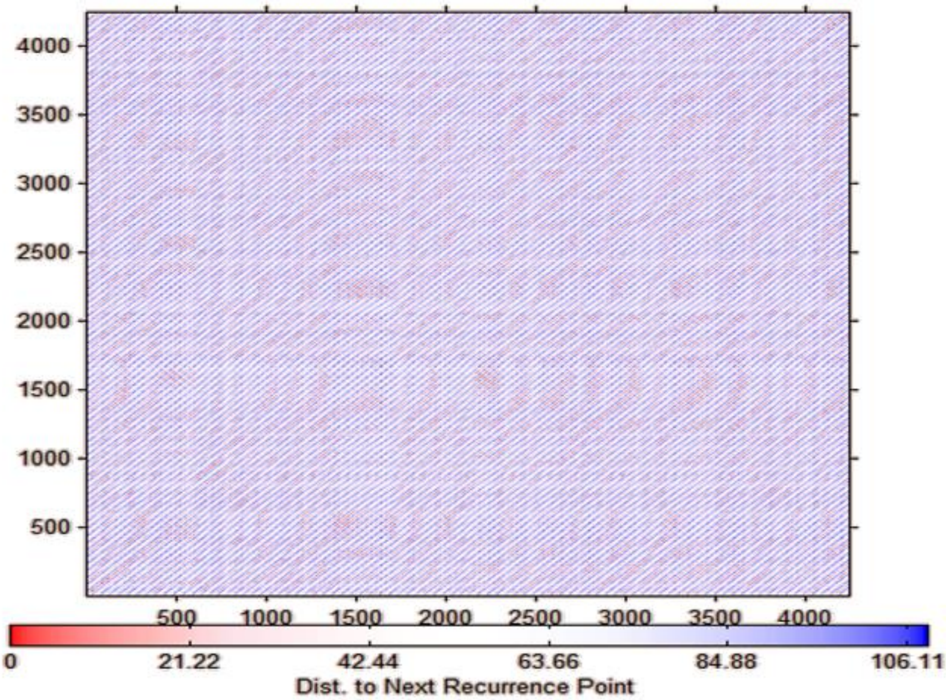

(a)

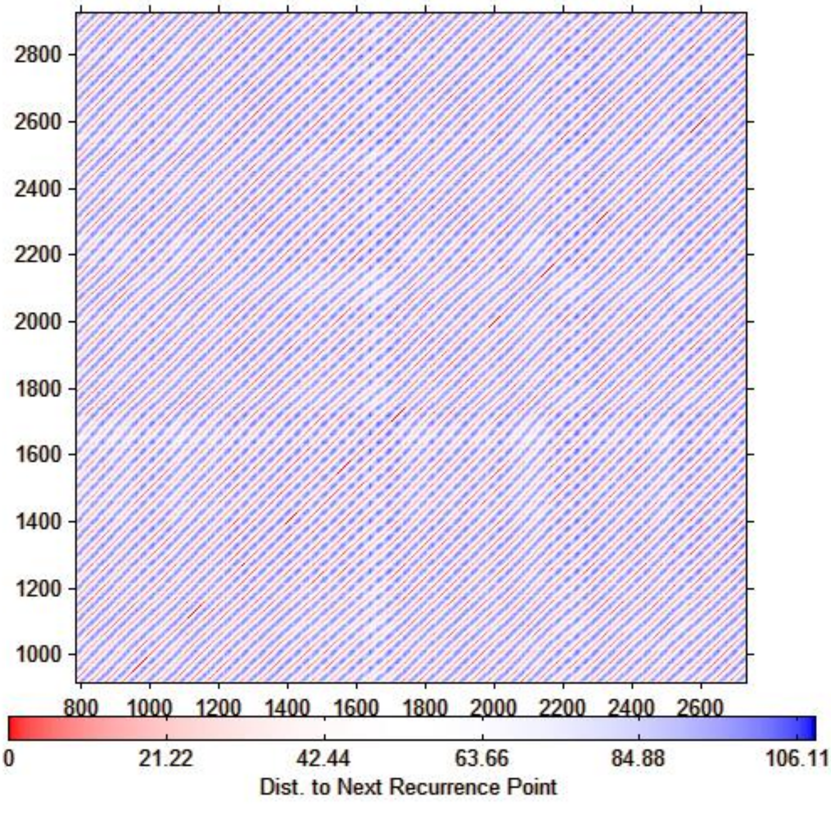

(b)

Figure 6.6 : The cross recurrence plot of (a) All data. (b) Zoomed for a better view.

7. MATHEMATICAL EQUATIONS AND NONLINEAR DYNAMICS

Nonlinear systems can be modelled by differential equations. The differential equations used for modeling a power system can be very complicated. It was previously stated that the ferroresonance circuit can be simplified and simulated as a parallel or series RLC circuit [2] In Chapter 4, the equivalent circuit for the power system was defined in details. At the end, the achieved equivalent circuit is a series RLC circuit. This chapter will focus on solving the differential equations of the RLC circuit with harmonic frequency components.

7.1 The Pre – Ferroresonance Case

The differential equation of the linear RLC circuit is given in Equation 7.1 [18].

$$\frac{d^2 i}{dt^2} + \frac{R}{L}\frac{di}{dt} + \frac{1}{LC} i(t) = \frac{\omega_s}{L} E\cos(\omega_s t) \tag{7.1}$$

Where

ω_s stands for supply angular frequency

E stands for peak supply voltage.

In the pre-ferroresonance region, the system is assumed to be operating as a linear circuit. Nevertheless, by spectral data analysis, it was observed that, the system did not only have the fundamental frequency, but also the 2nd harmonic frequency component of fundamental frequency which is 100 Hz. The 2nd harmonic is an indicator that the behavior of nonlinear system depends on the initial conditions of the system and even operating under healthy conditions, the system still has nonlinear properties. By comparing the amplitudes of the frequency components, it is found out that the 2nd fundamental frequency is 7.5 % of the fundamental frequency. That ratio will be used for calculating the driving force of the system. The right hand side of equation 7.1 will be modified according to the harmonic frequency components.

The R-L-C parameters will be brought from the equivalent circuit values. It is clear that, X_L and X_C are affected by the change of frequency where;

$$X_L = 2\,\pi\, f\, L \quad \textbf{(7.2)}$$

$$X_C = 2\,\pi\, f\, C \quad \textbf{(7.3)}$$

From the equivalent circuit given in Figure 4.2, it is clearly seen that, the only capacitance of the system is the power line capacitance, which is $2.082*10^{-6}$ F. The equivalent circuit parameters calculated for 50 Hz and 100 Hz are given in Equations 7.4 and 7.5 respectively.

$$Z_{eq50} = 0.0042+0.8891j \quad \textbf{(7.4)}$$

$$Z_{eq100} = 0.0042 + 1.7781j \quad \textbf{(7.5)}$$

The equivalent circuits are calculated as capacitance circuits. However, the differential equation also seeks for an inductance value. The equivalent circuit equations are modified by adding and subtracting the XC value to the equations. The modified equations are given in Equations 7.6 and 7.7.

$$Z_{eq50} = 0.0042+0.8898j-6.5410^{-4}j \quad \textbf{(7.6)}$$

$$Z_{eq100} = 0.0042 + 1.7794j-0.0013j \quad \textbf{(7.7)}$$

It is clear that the values of the equivalent impedances are not changed. The impedances are calculated with respect to these inductance values. The differential equations are given in Equations 7.8 and 7.9 separately.

$$\frac{d^2 i}{dt^2} + \frac{0.0042}{2.082\ 10^{-6}}\frac{di}{dt} + \frac{1}{2.082\ 10^{-6}\ 0.0028}i(t) = \frac{2\pi 50}{2.082\ 10^{-6}}\frac{15.75\ 10^{3}\sqrt{2}}{\sqrt{3}}cos(2\pi\ 50t) \quad \textbf{(7.8)}$$

$$\frac{d^2 i}{dt^2} + \frac{0.0042}{2.082\ 10^{-6}}\frac{di}{dt} + \frac{1}{2.082\ 10^{-6}\ 0.0028}i(t) = 0.00750\ \frac{2\,\pi\ 100}{2.082\ 10^{-6}}\frac{15.75\ 10^{3}\ \sqrt{2}}{\sqrt{3}}cos(2\pi\ 100t) \quad \textbf{(7.9)}$$

A space harmonic approximation will be adapted for modeling the equivalent circuits [109]. According to this approximation, the equivalent circuits can be connected in parallel to each other.

These two harmonic frequency circuits are connected in parallel and the achieved R-L-C parameters are calculated as:

R=0.0021 Ω;

L=1.041 10^6 H;

C=0.0056 F.

The modified differential equation is given in Equation 7.10.

$$\frac{d^2i}{dt^2}+\frac{0.0021}{1.041\ 10^6}\frac{di}{dt}+\frac{1}{1.041\ 10^6\ 0.0056}i(t)$$
$$=\frac{2\,\pi\,50}{1.041\ 10^6}\frac{15.75\ 10^3\sqrt{2}}{\sqrt{3}}cos(2\,\pi\,50t)$$
$$+\,0.0750\frac{2\pi\,100}{1.041\ 10^6}\frac{15.75\ 10^3\sqrt{2}}{\sqrt{3}}cos(2\,\pi\,100t) \qquad \textbf{(7.10)}$$

The phase portrait obtained by solving the differential equation is given in Figure 7.1.

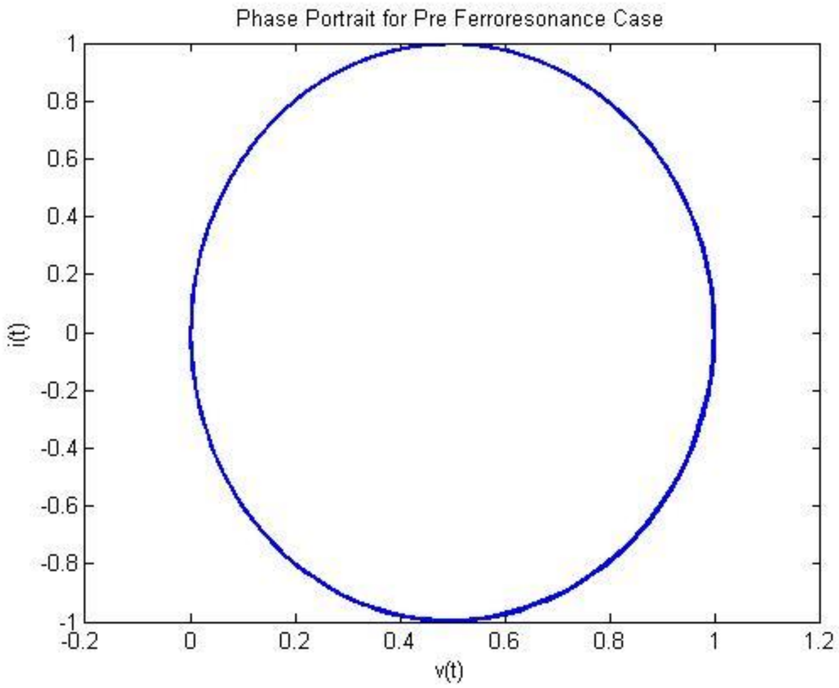

Figure 7.1 : The phase portrait obtained by solving the differential equation.

Despite that the system has the 2nd harmonic of the fundamental frequency, it can be observed from the phase portrait that the fundamental frequency is dominant. In the 5th chapter, the phase portraits constructed from the observed data were given in Figure 5.10 and Figure 5.11. Also in Figure 7.2, the phase portrait constructed from the collected data of flux and voltage is given. Although, the shapes of phase portraits are slightly different from each other, it is clear that they all indicate that the system is operating with the fundamental frequency. The cause of the difference is that the signals are derivatives of each other.

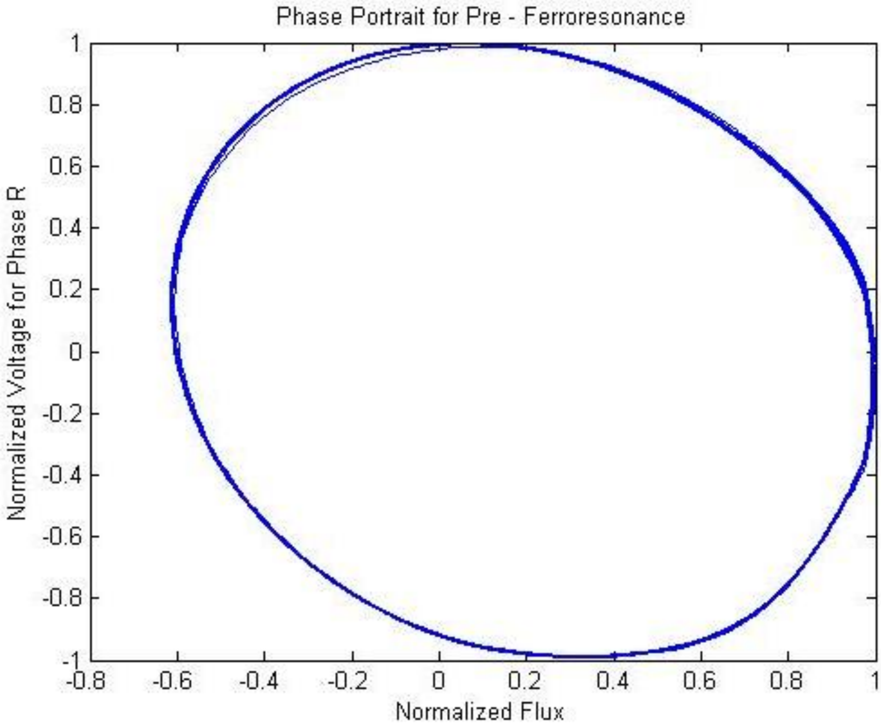

Figure 7.2 : Phase portrait for pre - ferroresonance.

By solving the differential equations, it is also verified that, before the occurrence of ferroresonance, the system is operating with the fundamental frequency. The differential equation of the RLC circuit is sufficient enough for modeling the system. For further studies, this equation can be modified in order to represent the nonlinear dynamics of the ferroresonance.

7.2 The Post – Ferroresonance Case

The current-flux diagram of a nonlinear inductance was given in the Chapter 2.. According to the graph, the most suitable correlation between the flux and current is given in Equation 7.11 [18].

$$i_m = a\phi + b\phi^n \quad \textbf{(7.11)}$$

Where,

Φ is the total flux linkage

i_m is the magnetizing current.

In this equation, $a\phi$ stands for the linear part and $b\phi^n$ stands for the nonlinear part of the hysteresis curve. N is chosen between 11-15 for modern transformers [18].

Replacing the nonlinear inductance by using ϕ-i_m characteristic, the differential equation of the RLC circuit is given in Equation 7.12.

$$\frac{d^2\phi}{dt^2} + \frac{1}{RC}\frac{d\phi}{dt} + \frac{1}{C}(a\phi + b\phi^n) = \omega_s E cos(\omega_s t) \qquad \textbf{(7.12)}$$

It should be considered that the polynomial representation for the nonlinear inductance is a good approximation but in some cases, it is not always possible to find a good polynomial fit if the exact B - H characteristic of the nonlinear inductance is unknown.

In the Seyitömer – Işıklar power line, the flux and the magnetizing current data for the transformer are collected from the simulation, but the polynomial approach for replacing the ϕ - i_m characteristic does not give an appropriate solution. Thus, a sigmoidal function is proposed which is given in Equation 7.13.

$$\phi = \frac{97}{1 + e^{(-i(t)+85)}} - 48 \qquad \textbf{(7.13)}$$

The actual ϕ-i characteristic and the sigmoidal function proposed are given in Figure 7.3. The proposed sigmoidal function is the best fitting curve among the other sigmoidal and polynomials. The sigmoidal function will be added to the linear differential equation of the RLC circuit in order to represent the nonlinearity. The achieved differential equation is given in Equation 7.14.

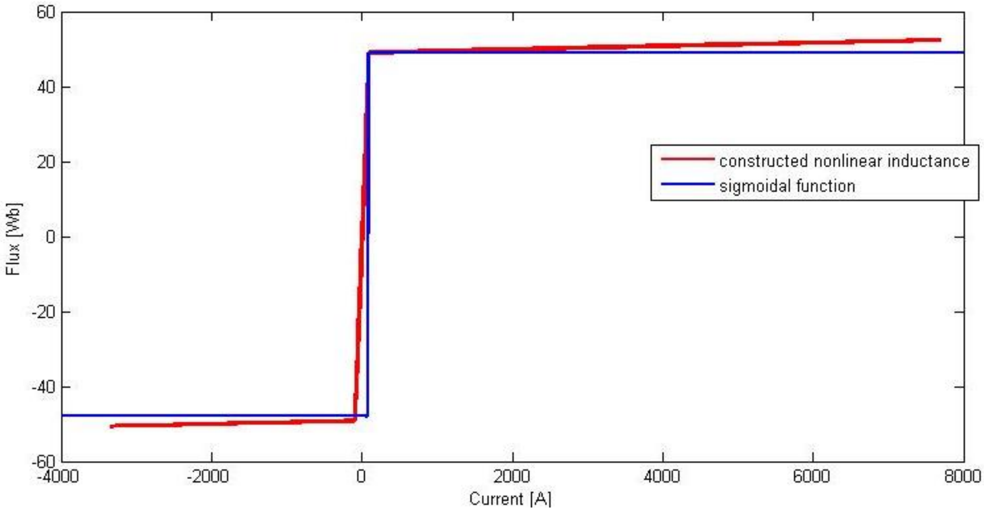

Figure 7.3 : The constructed nonlinear inductance and the sigmoidal function.

$$\frac{\omega_s \mathrm{E}\cos(\omega_s t)}{\mathrm{L}} = \left(\frac{97}{1+\mathrm{e}^{(-i(t)+85)}} - 48\right) + \frac{\mathrm{R}}{\mathrm{L}}\frac{\mathrm{di(t)}}{\mathrm{dt}} + \frac{1}{\mathrm{LC}}\mathrm{i(t)} + \frac{\mathrm{d}^2\mathrm{i}}{\mathrm{dt}^2} \qquad \textbf{(7.14)}$$

The equivalent circuit values for fundamental case of ferroresonance are given in Equation 7.15. The complete differential equation is given in Equation 7.16.

$$Z_{eq50} = 0.0071 + 1.0892j\text{-}6.54\ 10^{-4}j \qquad \textbf{(7.15)}$$

$$\frac{d^2 i}{dt^2} + \frac{0.0071}{1.0892}\frac{di}{dt} + \frac{1}{6.54\ 10^{-4}\ 1.0892} i(t) + \left(\frac{97}{1+\mathrm{e}^{(-i(t)+85)}} - 48\right) = \frac{2\,\pi\,50}{1.041\ 10^6}\frac{15.75\ 10^3\sqrt{2}}{\sqrt{3}}\cos(2\pi\,50t) \qquad \textbf{(7.16)}$$

For simulating the post-ferroresonance region, the load will be removed which will affect the equivalent impedance value of the circuit.

First of all, the differential equation is solved by using the fundamental frequency of 50 Hz as driving frequency to ensure that the sigmoidal function is representing the nonlinear inductance. In Figure 7.4, the phase portrait constructed from the solutions of the differential equation is given.

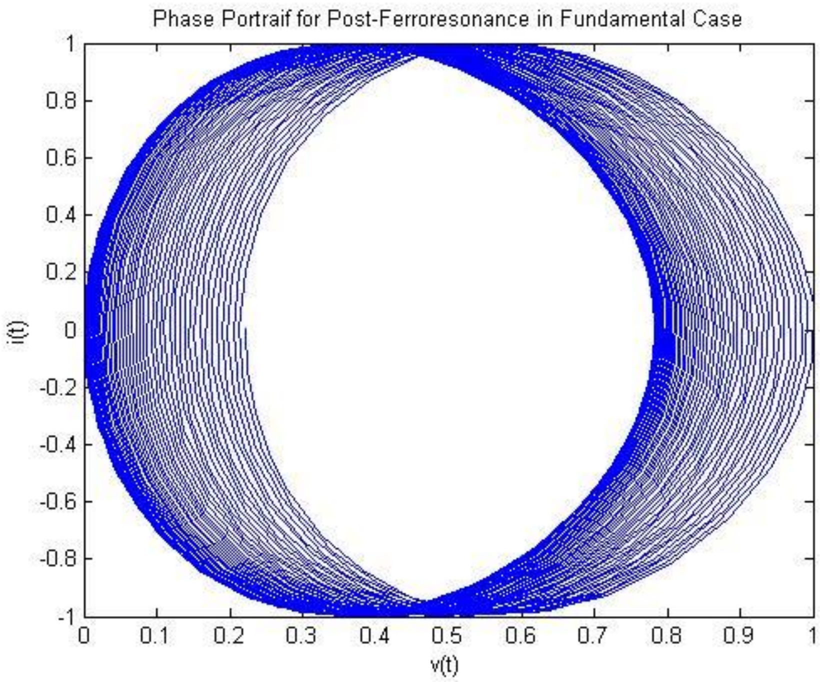

Figure 7.4 : Phase portrait for post ferroresonance in the fundamental case.

In Figure 7.5, the phase portrait for the post-ferroresonance case, plotted by the collected data from the simulation is given.

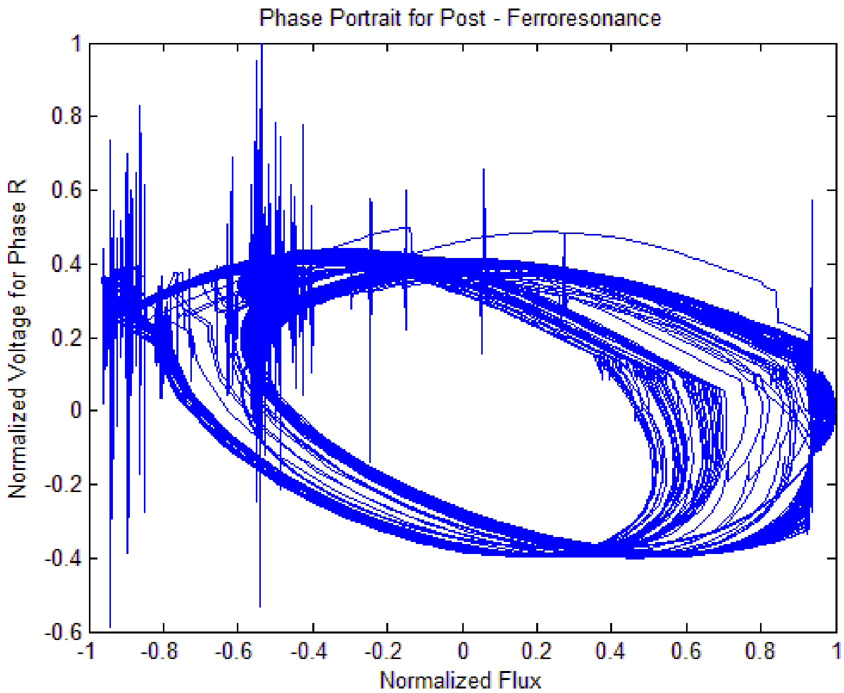

Figure 7.5 : Phase portrait of the simulation data for the post - ferroresonance.

In Figure 7.5, it is possible to see the effects of simulation noise and the harmonic frequency components. On the other hand, by comparing the phase portraits, it can be observed that the sigmoidal function is quite successful representing the nonlinear inductance. For further calculations focusing on sub-harmonic and quasi-periodic ferroresonance modes, the sigmoidal function will be utilized for modeling the nonlinear inductance.

It is not possible to split the data into the sub-harmonic and quasi-periodic regions but the modified differential equation will be used for verifying the steady state modes of ferroresonance.

7.2.1 The sub-harmonic ferroresonance mode

By using MRWA, it was concluded that, harmonic frequency components at 10 Hz, 12.5 Hz and 25 Hz were observed. The right hand side of the differential equation will be updated according to these frequency components with respect to their weights. In Table 7.1, the weights for the harmonic frequency components are given.

Table 7.1 : Weights of the sub harmonic frequency components.

Frequency (Hz)	Weight
10 Hz	0.1661
12.5 Hz	0.0814
25 Hz	0.1181
50 Hz	1

The RLC equivalent is calculated from the parallel connection of each circuit. The equivalent impedance values for the circuits are given in Equations 7.17-7.19

$$Z_{eq10} = 0.0070 + 0.2180j \quad \textbf{(7.17)}$$

$$Z_{eq12.5} = 0.0070 + 0.2725j \quad \textbf{(7.18)}$$

$$Z_{eq25} = 0.0070 + 0.5450j \quad \textbf{(7.19)}$$

By the parallel connection of these sub-harmonic circuits and the fundamental circuit, the resulting differential equation is given in Equation 7.20.

$$\frac{d^2i}{dt^2} + \frac{1.75\ 10^{-3}}{0.771\ 10^{7}}\frac{di}{dt} + \frac{1}{0.771\ 10^{7}\ 0.013}i(t) + \left(\frac{97}{1+\mathrm{e}^{(-i(t)+85)}} - 48\right) =$$
$$\frac{15.75\ 10^{3}\sqrt{2}}{0.771\ 10^{7}\sqrt{3}}[\left(2\,\pi 50\ cos(2\,\pi\ 50t)\right) + \left(0.1661\ 2\pi\ 10cos(2\pi\ 10t)\right) +$$
$$\left(0.0814\ 2\,\pi\ 12.5\ cos(2\,\pi\ 12.5\ t)\right) + \left(0.1181\ 2\pi\ 25\ cos(2\,\pi\ 25t)\right)] \quad \textbf{(7. 20)}$$

The phase portrait for the sub harmonic frequency components is given in Figure 7.6. The phase portrait clearly indicates that the differential equation represents the sub-harmonic case for post-ferroresonance region. The outer circle stands for the fundamental frequency whereas the inner circles stand for other frequency components.

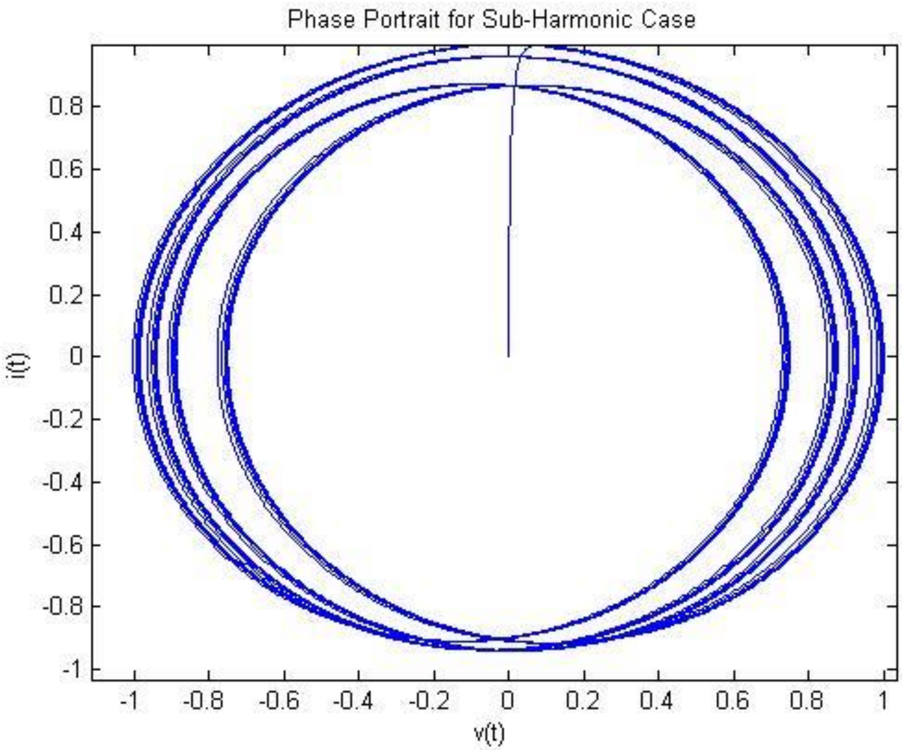

Figure 7.6 : Phase portrait for sub-harmonic case.

7.2.2 The quasi-periodic ferroresonance mode

It was previously stated that ferroresonance caused the quasi-periodic harmonic frequency components with 130 Hz and 193 Hz. The weights for the frequency components are given in Table 7.2.

Table 7.2 : Weights of the quasi periodic harmonic frequency components.

Frequency (Hz)	Weight
130 Hz	0.3630
193 Hz	0.1381
50 Hz	1

The equivalent impedances for the quasi-periodic circuits are given in Equations 7.21 and 7.22.

$$Z_{eq130} = 0.0077 + 2.8337j \quad \textbf{(7.21)}$$

$$Z_{eq193} = 0.0088 + 4.2941j \quad \textbf{(7.22)}$$

As a result of the parallel connection of the quasi-periodic and the fundamental circuits, the achieved differential equation is given in Equation 7.23.

$$\frac{d^2i}{dt^2} + \frac{2.60\ 10^{-3}}{1.028\ 10^7}\frac{di}{dt} + \frac{1}{1.028\ 10^7\ 0.010}i(t) + \left(\frac{97}{1+\mathrm{e}^{(-i(t)+85)}} - 48\right) =$$
$$\frac{15.75\ 10^3\ \sqrt{2}}{1.028\ 10^7\ \sqrt{3}}\left[\left(2\pi\ 50\ cos(2\ \pi\ 50t)\right) + \left(0.3630\ 2\pi\ 130\ cos(2\pi\ 130t)\right) +\right.$$
$$\left.\left(0.1381\ 2\pi\ 193\ cos(2\pi\ 193t)\right)\right] \quad \textbf{(7.23)}$$

The phase portrait of the differential equation is given in Figure 7.7. The quasi-periodic oscillations cause a torus shaped phase portrait. From the phase portrait, it is seen that the trajectories are following spiral directions and forming a torus.

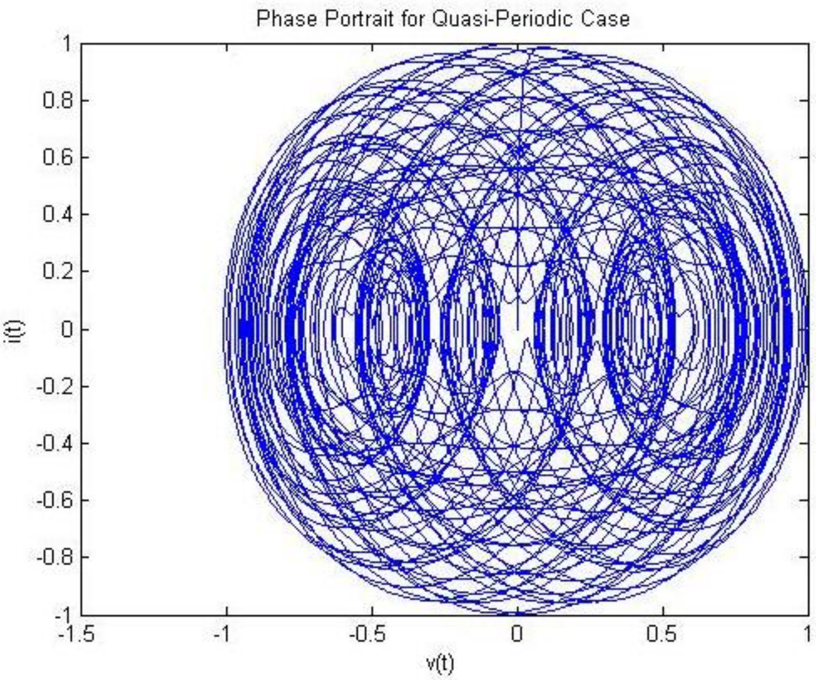

Figure 7.7 : Phase portrait for quasi-periodic case.

The most important outcome of this chapter is the replacement of the polynomial approximation of the hysteresis curve with another nonlinear function. It is clearly shown that the sigmoidal function is very successful for representing the hysteresis curve of the transformer. In cases where achieving the real parameters of a transformer in an actual power system is impossible, a suitable sigmoidal function can be utilized for representing the hysteresis curve.

The research in the literature is not focusing on the entire power system, but only the transformer. On the other hand, the power system should be taken into the consideration as a whole from generation to distribution. It is definitely realized that the equivalent circuit for pre and post ferroresonance regions are different from each other. The earlier studies showed the steady state caused by the ferroresonance affecting the transformer. This new differential equation approximation stands for the entire power system and all the system parameters affecting the ferroresonance are taken into consideration.

8. CONCLUSIONS AND DISCUSSIONS

Power system operations in good conditions are very important both for utilities and customers. Deenergizing of a small part of the power system for even a very short time period can cause huge economic losses and many customers to be out of energy. All the equipment of a power system are potential fault locations. The occurrence of these faults should be analyzed carefully and special precautions should be considered in order to prevent these faults. However, it is not always possible to prevent the occurrence of these faults due to the nature of the system. Ferroresonance is a good example to these faults which is defined as the interaction between a nonlinear inductance and a capacitance in the power system. Although it is a rare process, the consequences are usually very destructive therefore it is important to understand the behavior of the phenomenon in order to prevent the occurrence.

Most important outputs of this study are as follows:

- This study focused on the ferroresonance phenomenon and its nonlinear dynamics. A part of the Turkish power system is chosen for ferroresonance studies and it is modelled using Matlab – SIMULINK software. There are many causes of ferroresonance like short circuits, capacitor or transformer switching, turning off the load suddenly. In the simulation, the load is suddenly removed and the effects are observed as overvoltages. It is also known that, besides overvoltages, ferroresonance also cause over – currents and harmonic frequency components. In this study STFT and MRWA are utilized in order to find the harmonic frequency components. STFT figured out that high frequency components are generated during the phenomenon but it did not give brief information whether the harmonics are sub harmonic, quasi periodic or chaotic. Therefore, MRWA is applied in order to limit the harmonic frequency components in certain frequency bands. The use of MRWA makes it possible to identify the characteristics of frequencies. In the sub harmonic frequency band 10 Hz, 12.5 Hz and 25 Hz frequency components are observed. As quasi periodic frequency components, $130 \pm \Delta f$ Hz and $193 \pm \Delta f$ Hz are detected.

- After identifying the frequency components, the equivalent circuit of the power system is calculated in order to simplify the system as an RLC circuit. Here, basic equivalent models for generators, transformers and the power line are used. Once the equivalent circuit is computed, the differential equation for the RLC circuit is used for identifying the nonlinear dynamics of ferroresonance. Although, an ordinary differential equation is sufficient to analyze the pre – ferroresonance case, it is observed that for the post – ferroresonance case, the nonlinearities should also be addressed. The differential equation is modified by adding a sigmoidal function in order to represent the nonlinear inductance, i.e. the transformer and phase portraits are plotted for having a better understanding about the nonlinear dynamics of ferroresonance in a power system.
- Well-known chaos indicator Lyapunov exponents are also used for a deep understanding of nonlinear dynamics. Lyapunov exponents are used for determining the chaotic behavior of the system but their calculation is not a straightforward process. In addition, real systems have very complicated differential equations and it is sometimes impossible to know these equations. For dealing with this problem some estimation methods using time series of the signal are proposed. One of these methods is utilized for estimating the largest Lyapunov exponent of the signal. LLE is estimated as greater than zero which is actually an indication of chaos. On the other hand, from the time series, it is known that the system is not in a chaotic mode therefore further investigations are performed. Recurrence plots of the signal are created and they expose that the system is not in a chaotic mode. Although LLE is very close to zero, it could not be possible to identify if it is real LLE or this deviation is a result of simulation noise. When dealing with Lyapunov exponents, it would be a wise idea to double-check the results with other decision tools.

Novelties in this study are as follows:

- The first novelty of the thesis is that the power system is modelled as a whole. In the literature, studies focused on the transformer and its parameters but the other components of the power system were ignored. For the first time, all components of the power system including the generator and the power line are taken into account. In addition to this all losses of the transformer are modelled by using the Tee – equivalent circuit. The model used in the thesis is the most comprehensive model of power system to study the ferroresonance phenomenon. This comprehensive model allows displaying all properties of ferroresonance.

- The second novelty of the thesis is using MRWA for identifying the harmonic frequency components. In previous studies, which really provided the necessary motivation for the thesis, CWT was used to understand the phenomenon. The main shortcoming of this method is that it could not define the sub harmonics and quasi periodic harmonics clearly. The usage of filter banks enables the identification of these harmonics and exact harmonic frequency components whicah are caused by ferroresonance are identified. The SIMULINK model is relatively easy to construct. Signal processing techniques can be used in the design process and the vulnerabilities of the power system can be identified before building up the actual system.
- The nonlinear dynamics of ferroresonance are studied through ordinary differential equations. According to the classical approach, the ODEs are constructed by using a polynomial nonlinear inductance model. For a new system, the parameters are very well – known and the polynomial approach can be very effective. On the other hand, especially for existing power systems, usually most of the parameters cannot be reached. In the simulation used for the thesis, the exact characteristic for the nonlinear inductance was not present and it was not possible to use a polynomial approach. In order to overcome this problem the nonlinear inductance is modelled by using a nonlinear function, which is sigmoidal. It is observed that the sigmoidal function is as successful as the polynomial function for modeling the nonlinearities that are brought by the transformer core. By solving the differential equations, the sub harmonic and quasi periodic oscillations, which are caused by ferroresonance, are shown clearly. The mathematical model approves the results of MRWA.

Two further studies are proposed. The first one is to build an analog circuit model which is identified in mathematical equations Through this it will be possible to prove the outcomes of nonlinear dynamics. On the actual circuit, it would also be possible to examine how the changes of parameters affect the occurrence of ferroresonance. The second proposed study is to collect actual power system data in collaboration with the local utility. The real system signal will be very useful to work on as it contains all necessary data about the power system. If a real time power system signal is presented, than the conditions drifting the system into the ferroresonance mode can be identified more clearly. The main problem is to find the exact data containing the ferroresonance operation mode as it is a very rare phenomenon.

REFERENCES

[1] **Saadat, B.** (1998). *Power System Analysis.* McGraw – Hill, New York City, NY.

[2] **Kieny, C.** (1991). Application of the bifurcation theory in studying and understanding the global behavior of a ferroresonant electric power circuit. *IEEE Transactions on. Power Delivery*, *6*(2), 866–872.

[3] **Ferracci, P.**(1998). *Cahier Technique No: 190 Ferroresonance.* Groupe Schneider, Paris, France.

[4] **Braun, D., Delfanti, M., Palazzo, M., Zich, R.** (2012). Harmonic Distortion in Power Stations Due to Ferroresonance. In APEMC. *Proceedings of Asia-Pacific Symposium on Electromagnetic Compatibility* Singapore, 21 -21 May.

[5] **Charalambous, C. A., Sturgess, J. P**.(2011). Frequency domain analysis of a power transformer experiencing sustained ferroresonance. *IET Generation Transmission Distribution*, *5*(6), 640 – 649.

[6] **Ben-Tal, A., Shein, D., Zissu,S.** (1999). Studying ferroresonance in actual power systems by bifurcation diagram. *Electric Power System Research, 49*(3), 175–183.

[7] **Hassan, S., Vaziri, M., Vadhva, S.** (2011). Review of Ferroresonance in Power Distribution Grids. In IRI. *Proceedings of IEEE International Conference on Information Reuse and Integration* , Las Vegas, USA, 3 – 5 August.

[8] **Mokryani,G., Siano, P., Piccolo, A.**(2010). Identification of ferroresonance based on S-transform and support vector machine. *Simulation. Modeling. Practice and. Theory*, *18*(9), 1412–1424.

[9] **Bo, Z., Tiecheng, L.** (2009). Application of Nonlinear Dynamic on Ferroresonance in Power System. In *IEEE Asia-Pacific Power Energy Engineering Conference,* Wuhan, China, 27 – 31 March.

[10**] Akinci, T. C., Ekren, N., Seker, S., Yıdırım, S.** (2013). Continuous wavelet transform for ferroresonance phenomena in electric power systems, *International Journal of Electrical Power and Energy Systems, 44*(1), 403–409.

[11] **Sanaye-Pasand, A. Mohseni, M., Farhangi, S., Rezaei-Zare, A., Iravani, R**. (2004). Effects of Initial conditions on Ferroresonance in Power Transformers Using Preisach Theory. In UPEC. *Proceedings of IEEE 39th International Universities Power Engineering Conference,* Bristol, United Kingdom, 6 – 8 September.

[12] **Rezaei-zare, A., Sanaye-pasand, M., Mohseni, H.** (2007). Analysis of ferroresonance modes in power transformers using Preisach-type

hysteretic magnetizing inductance, *IEEE Transactions on Power Delivery*, *22*(2), 919–929.

[13] **Moses, P. S., Masoum, M. A. S.** (2010). Sensitivity of Ferroresonance Simulations to Model Parameters and Initial Conditions. In AUPEC. *Proceedings of IEEE 20th Australasian Universities Power Engineering Conference* University of Canterbury New Zealand, 5 -8 December.

[14] **Rezaei-zare, A., Iravani, R., Sanaye-pasand, M.** (2009). Impacts of transformer core hysteresis formation on stability domain of ferroresonance modes, *IEEE Transactions on Power Delivery*, *24*(1), 177 – 186.

[15] **Chunbao, W., Lijun, T.** (2011). A Study on Factors Influencing Ferroresonance in Distribution System. In DRPT. *Proceedings of IEEE 4th International Conference on Electric Utility Deregulation and Restructuring and Power Technologies,* International Academic Center of Shandong University Hotel, China 6 – 9 July.

[16] **Al-Anbarri, K., Ramanujam, R., Saravanaselvan, R., Kuppusamy, K.** (2003). Effect of iron core loss nonlinearity on chaotic ferroresonance in power transformers, *Electric Power Systems Research*, *65*(1), 1-12.

[17] **Mozaffari, S**. (1996). Chaotic Ferroresonance in Power Transformers, *PhD Thesis* , The University of British Columbia, Vancouver, Canada.

[18] **Marti, J. R., Soudack, A. C.** (1991). Ferroresonance in power systems: fundamental solutions, *IEE Proceedings - C Generation Transmission Distribution*, *138*(4), 321 – 329.

[19] **Kang, Y. C., Lee, B. E., Zheng, T. Y., Kim, Y. H., Crossley, P. A.** (2010). Analytical Analysis of PT Ferroresonance in the Transient-State," in DPSP. *Proceedings of the 10th IET International Conference on Developments in Power System Protection: Managing the Change*, Manchester, United Kingdom, March 29 – April 1.

[20] **Nakhla, M., Vlach, J.** (1976). A piecewise harmonic balance technique for determination of periodic response of nonlinear systems, *IEEE Transmission Circuits Systems*, *23*(2), 85–91.

[21] **Kim, N. C., Perkins, W. J.** (2003). Harmonic balance/Galerkin method for non-smooth dynamic systems, *Journal of Sound and Vibration*, 261,213–224.

[22] **Ben Amar, F., Dhifaoui, R**. (2011). Study of the periodic ferroresonance in the electrical power networks by bifurcation diagrams, *International Journal of Electrical Power and Energy Systems, 33*(1), *61-85.*

[23] **Harmonic Balance Method** (n. d.). In *Wikipedia* Date retrieved 12. 01. 2014, address: http://en.wikipedia.org/wiki/Harmonic_balance

[24] **Galerkin Method (**n. d.). In *Wikipedia* Date retrieved 12. 01. 2014, address: http://en.wikipedia.org/wiki/Galerkin_method

[25] **Mokryani, M. R., Haghifam, G.** (2007). Identification of Ferroresonance Based On Wavelet Transform And Artificial Neural Networks. In

Australasian Universities Power Engineering Conference, Perth, Australia, 9 – 12 December.

[26] **Radmanesh, H., Fathi, S. H., Rostami, M., Kamali, R.** (2011). Controlling Ferroresonance Oscillations in Potential Transformer : part II. In ICEE. *Proceedings of IEEE 19th Iranian Conference on Electrical Engineering,* AmirKabir University of Technology, Iran, 17 -19 May.

[27] **Huang, Q., Sima, Y., Yang, W.** (2011). A Module-Based Scalable Identification System for Power System Overvoltage Events. In DRPT. *Proceedings of* IEEE *4th International Conference on Electric Utility Deregulation and Restructuring and Power Technologies,* International Academic Center of Shandong University Hotel, China, 6 – 9 July.

[28] **Horak, J.** (2004). A Review of Ferroresonance. In *proceedins of IEEE 57th Annual Conference for Protective Relay Engineers*, Texas A&M University, USA, March 30 - April 1.

[29] **Transformer Committee of IEEE Power Engineering Society** (2008). IEEE Guide for Application of Transformer Connections in Three-Phase Distribution Systems, date retrivied 05.01.2014, address: http://ieeexplore.ieee.org/xpl/mostRecentIssue.jsp?punumber=2652

[30] **Huang, S. J., Hsieh, C. H.** (2013). Relation analysis for ferroresonance of bus potential transformer and circuit breaker grading capacitance," *International Journal of Electrical Power and Energy Systems,* 51, 61–70.

[31] **Laohacharoensombat, K., Jaruwattanadilok,S.,Tuitemwong, K., Wattanasakpubal, C., Kleebmek,K.** (2004). Case Study of Ferroresonance in 33 kV Distribution Network of PEA Thailand. In TENCON. *Proceedings of IEEE Region 10 Conference,* Chiang Mai, Thailand, 21 -24 November.

[32] **Olguín-Becerril, M. A., Angeles-Camacho, C., Fuerte-Esquivel, C. R.** (2014). Electrical power and energy systems ferroresonance in sub harmonic 3rd mode in an inductive voltage transformer , a real case analysis, *International Journal of Electrical Power and Energy Systems, 61*, 318–325.

[33] **Zhang, B., Tiecheng, L.** (2009). On the Use of Wavelet Decomposition for Ferroresonance Detection in Power System. In *IEEE Asia-Pacific Power Energy Engineering Conference,* Wuhan, China, 27 – 31 March.

[34] **Guo, P. Y. , Li, C. Z., Yan, S., Zhang, Y. J.** (2011). Application of Wavelet Transform in Ferroresonance Detection. In AIMSEC. *Proceedings of IEEE 2nd International Conference on Artificial Intelligence, Management Science and Electronic Commerce*, Fengleyuan Hotel, China, 8 – 10 August.

[35] **Mokryani, G., Haghifam, M. R., Latafat, H., Aliparast, P., Abdolahi, A.** (2009). Wavelet Based Kernel Fisher Classifier For Ferroresonance Identification. In ISAP. *Proceedings of IEEE 15th International*

Conference on Intelligent System Applications to Power Systems, Universidade Positivo, Brazil, 8 – 12 November.

[36] **Mokryani, G., Haghifam, M. R.** (2008). Application of Wavelet Transform and MLP Neural Network for Ferroresonance Identification. In IEEE PES General Meeting, *Proceedings of the Conversion and Delivery of Electrical Energy in the 21st Century,* Pittsburgh, USA, 20 - 24 July.

[37] **Beheshtaein, S.** (2012). Application of Wavelet-base Method and DT in Detection of Ferroresonance from Other Transient Phenomena. In INISTA. *Proceedings of the International Symposium on Innovations in Intelligent Systems and Applications*, Trabzon, Turkey, 2 – 4 July.

[38] **Akıncı, T. Ç.** (2009). Güç Sistemlerinde Ferrorezonans Olayının Spektral ve Dalgacik Analizi Yöntemleriyle Belirlenmesi, *PhD Thesis*, Marmara University, İstanbul, Turkey.

[39] **Slow Transients Task Force of the IEEEWorking Group on Modeling and Analysis of Systems Transients Using Digital Programs**, (2000). Modeling and Analysis Guidelines for Slow Transients — Part III : The Study of Ferroresonance, *IEEE Transactions on Power Apparatus and Systems, 15*(1), 255–265.

[40] **Ferroresonance in ElectricityNnetworks** (n. d.). In *Wikipedia*, Date retrieved: 18. 11.201, address: http://en.wikipedia.org/wiki/Ferroresonance_in_electricity_networks#cite_note-valverde-2

[41] **Mork, B. A.** (2006). Understanding and Dealing With Ferroresonance. In *Minnesota Power Systems Conference*, University of Minnesota, USA, 7 – 9 November.

[42] **Rüdenberg, R.** (1950). *Transient Performance of Electric Power Systems*. McGraw – Hill, New York City, NY.

[43] **Robbins, W. C., and Miller, A. H**.(2013). *Circuit Analysis: Theory and Practice.* Cengage Learning, New York City, NY.

[44] **Valverde, V., Mazón, A. J., Zamora, I., Buigues, G.** (2007). Ferroresonance in Voltage Transformers : Analysis and Simulations. In *International Conference on Renewable Energies and Power Quality*, Sevilla, Spain 28 – 30 March.

[45] **Miličević, K., Emin, Z.** (2009). Impact of Initial Conditions on the Initiation of Ferroresonance, *International Journal of Electrical Power and Energy Sytems, 31*(4), 146–152.

[46] **Rioual, M., Sicre, C.** (2001). Energization of a No-Load Transformer for Power Restoration Purposes : Impact of the Sensitivity to Parameters. In IPST '09. *Proceedings of the International Conference on Power Systems Transients,* Rio de Janeiro, Brazil, 24 – 28 June.

[47] **Roy, M.,. Roy, C. K.** (2009). A Study on Ferroresonance and Its Depedence on Instant of Switching Angle of the Source Voltage. In 3rd *International Conference on Power Systems,* Kharagpur, India, 27 -29 December.

[48] **Sameti, M., Soudack, A. C.** (1997). Effect of initial conditions on chaotic ferroresonance in power transformers, *IEE Proceedings C Generation Transmission Distribution*, *144*(5), 456–460.

[49] **Roy, M.,. Roy, C. K.** (2009). A Study on Ferroresonance with a Varying Initial Conditions Using a Nonlinear Model of Transformer. In ICPS '09. *Proceedings of the International Conference on Power Systems*,Kharagpur, India, 27 -29 December.

[50] **Araujo, A. E. A., Soudack, A. C., Marti, J. R.** (1993). Ferroresonance in power systems: chaotic behaviour, *IEE Proceedings C Generation Transmission. Distribution*, *140*(3), 237- 240.

[51] **Swift G. W., Cos, E.** (1969). An analytical approach to ferroresonance," *IEEE Transactions on Power Apparatus and Systems, 88*(1), 42–46.

[52] **Mulad, M. M., Fahmy, M. S.,** (1980). An analytical investigation of a ferroresonant circuit, *IEEE Transactions on Magnetics*, *16*(2), 465–468.

[53] **Maklad, M., Zaky, A.** (1976). Multimodal operation of a ferroresonant circuit with quintic nonlinearity, *IEEE Transactions on Magnetics*, *12*(4), 380–384.

[54] **Li, Y., Shi,W., Li, F.** (2006). Novel analytical solution to fundamental ferroresonance — part I : power frequency, *IEEE Transactions on Power Delivery, 21*(2), 788–793.

[55] **Li, Y., Shi,W., Li, F.** (2006). Novel analytical solution to fundamental ferroresonance—part II: criterion and elimination," *IEEE Transactions on Power Delivery, 21*(2), 794–800.

[56] **Piasecki,W., Florkowski, M., Fulczyk, M., Mahonen, P**. (2007). Mitigating ferroresonance in voltage transformers in ungrounded MV networks, *IEEE Transactions on Power Delivery, 22*(4), 2362–2369.

[57] **Pasand – Sanaya, M., Rezaei-Zare, A., Mohseni, H., Farhangi, S., Iravani,R.** (2006). Comparison of Performance of Various Ferroresonance Suppressing Methods in Inductive and Capacitive Voltage Transformers. In *IEEE Power India Conference*, New Delhi, India, 10 -12 April.

[58] **Abbasi, A., Seifi, A.** (2009). Fast and perfect damping circuit for ferroresonance phenomena in coupling capacitor voltage transformers, *Electric Power Components and Systems*, *37*(4), 393–402.

[59] **Durbak, D. W.** (2004) . Ferroresonance damping device solves Amtrak's problem, *Shaw Power Technologies Inc., Newsletters*, 96, 1 -2.

[60] **Piasecki, W. Stosur, M., Florkowski, M., Fulczyk, M., Lewandowski, B.** (2009). Mitigating Ferroresonance in HV Inductive Transformers. In IPST '09. *Proceedings of the International Conference on Power Systems Transients,* Rio de Janeiro, Brazil, 24 – 28 June

[61] **Shahabi, M., Babazadeh, S., Shirvani, D., Purrezagholi, R. E.** (2009) Mitigating Ferroresonance in Coupling Capacitor Voltage Transformers with Ferroresonance Suppressing Circuits. In IEEE EUROCON. *Proceedings of IEEE Region 8 Conference,* Saint Petersburg, Russia, 18 - 23 May.

[62] **Radmanesh, H., Gharehpetian, G. B.** (2013). Ferroresonance suppression in power transformers using chaos theory," *International Journal on Electrical Power and Energy Systems*, *45*(1), 1–9.

[63] **Radmanesh, H., Gharehpetian, G. B., Fathi, H.** (2012). Ferroresonance of power transformers considering non-linear core losses and metal oxide surge arrester effects, *Electric Power Components and Systems*, *40*(5), 463–479.

[64] **Akansu, R. A., Haddad, A. N.(**2001). *Multiresolution Signal Decomposition, Transforms, Subbands, Wavelets.* Academic Press, San Diego, CA.

[65] **Chan, C., Peng, A. K**. (2003) *Wavelets for Sensing Technologies*. Artech House Inc., Boston, MA.

[66] **Gopinath, C. S., Burrus, R. A**. (1992). Wavelets A Tutorial in Theory and Applications, C. K. Chui (Ed.), *Wavelet Transforms and Filter Banks* (pp. 603 - 654) Academic Press, Boston, MA.

[67] **Hubbard, B.B.** (1998). *The World According to Wavelets : The Story of a Mathematical Technique in the Making*. A.K. Peters, MA.

[68] **Wavelet** (n. d.). In *Wikipedia,* Date retrivied 20.10.2014 address: http://en.wikipedia.org/wiki/Wavelet#History

[69] **Daubechies, I.** (1992). *Ten Lectures on Wavelets*. SIAM, Philadelphia.

[70] **Vetterli, J., Kovacevic, M.**(1995). *Wavelets and Subband Coding*, Prentice Hall, Englewood Cliffs, NJ.

[71] **Graps, A.** (1995). An introduction to wavelets, *IEEE Computer Science Engineering, 2*, 50–61.

[72] **Abbate, P. K., DeCusatis, A., Das, C. M.** (2002). *Wavelets and subbands Fundamentals and Applications*. Birkhauser, Boston, MA.

[73] **Valens, C**. (1999). *A Really Friendly Guide to Wavelets.* Date retrivied: 10.10.2014, address: https://www.cs.unm.edu/~williams/cs530/arfgtw.pdf

[74] **Kaiser, G**. (1994). *A Friendly Guide to Wavelets*. Birkhauser, Boston, MA.

[75] **Lyapunov Exponent** (n. d.). In *Scholarpedia*, Date retrivied: 25.12.2013, address: http://www.scholarpedia.org/article/Lyapunov_exponent

[76] **Meador, C. E.** (2011). *Numerical Calculation of Lyapunov Exponents for Three-Dimensional Systems of Ordinary Differential Equations*. Date retrivied:20.12.2013,address:http://mds.marshall.edu/cgi/viewcontent.cgi?article=1105&context=etd

[77] **Wolf, A., Swift, J. B., Swinney, H. L.,Vastano, J. A.** (1985). Determining Lyapunov exponents from a time series, *Physica D Nonlinear Phenomena*, *16*(3), 285–317.

[78] **Nayfeh, B., Balachandran, A.H.(**1995). *Applied Nonlinear Dynamics Analytical, Computational and Experimental Methods*. John Wiley & Sons Ltd, New York City, NY.

[79] **Chapman, S. J.**(1998) *Electric Machinery Fundamentals*, McGraw – Hill, Singapore.

[80] **Moses, P. S., Masoum, M. A. S.** (2009) “Modeling Ferroresonance in Asymmetric Three-Phase Power Transformers. In AUPEC 2009. *Proceedings of IEEE 19th Australasian Universities Power Engineering Conference* Adelaide, Australia, 27 -30 September.

[81] **Faulkenberry, W., Coffer, L. M**. (1996). *Electrical Power Distribution and Transmission*: Prentice Hall, New Jersey, NJ.

[82] **Strogatz, S. H.** (2000). *Nonlinear Dynamics and Chaos*. Westview Press, Cambridge.

[83] **Harb, M. S., Widyan, A.M.** (2004). Chaos and bifurcation control of SSR in the IEEE second benchmark model, *Chaos, Solitons & Fractals, 21*(3), 537–552.

[84] **Unnu, S. Y., Şeker, S.** (2014). Multi-resolution wavelet analysis for ferroresonance phenomena in power systems, *Electrical Power Components and Systems, 42*(6), 567–575.

[85] **Attractor Reconstruction.** (n. d.). In *Scholarpedia*, Date retrivied: 15.03.2014, address: http://www.scholarpedia.org/article/Attractor_reconstruction

[86] **Takens, F.** (1981). Detecting Strange Attractors in Turbulence, *Lecture Notes Mathematics*, 898, 366–381.

[87] **Mutual Information.** (n. d.). In *Scholarpedia*, Date retrivied: 20.03.2014, address: http://www.scholarpedia.org/article/Mutual_information

[88] **Mutual Information.** (n. d.).In *Wikipedia*, Date retrivied: 29.03.2014, address: http://en.wikipedia.org/wiki/Mutual_information

[89] **Fraser, H., Swinney, A. M.** (1986). Independent coordinates for strange attractors from mutual information, *Physical Reviews A*, *33*,1134–1140.

[90] **Auto Correlation.** (n. d.). In *Wikipedia*, Date retrivied: 20.03.2014, address: http://en.wikipedia.org/wiki/Autocorrelation

[91] **Kim, H. S., Eykholt, R., Salas, J. D.** (1999). Nonlinear dynamics, delay times, and embedding windows, *Physica D Nonlinear Phenomena, 127*(1-2), 48–60.

[92] **Yılmaz, D., Güler, N. F.** (2006). Kaotik zaman serisinin analizi üzerine bir araştırma, *Gazi Üniversitesi Mühendislik Mimarlık Fakültesi Dergisi, 21*(4), 759–779.

[93] **Merkwirth,C., Parlitz, U., Wedekind, I., Engster D., Lauterborn, W.** (2009). *MATLAB OpenTSTool User Manual*, Date retrivied: 12.04.2014, address: http://www.physik3.gwdg.de/tstool/manual.pdf Drittes Physikalisches Institut Universität Göttingen, Germany.

[94] **Boker, S. M.** (1996). Linear and Nonlinear Dynamical Systems Data Analytic Technique and an Application to Developmental Data, *PhD Thesis*, University of Virginia, Charlottesville, USA.

[95] **Kennel, M.B., Abarbanel, H. D.** (2002). False neighbours and false strands: A reliable minimum embedding dimension algorithm, *Physical Reviews E, 66*(2), 1-18.

[96] **Kennel, M. B., Brown, R., Abarbanel, H. D.** (1992). Determining embedding dimensions for phase-space reconstrucation using a geometrical construction, *Physical Reviews A*, *45*(6), 3403 – 3411.

[97] **Cao, L.** (1997). Practical method for determining the minimum embedding dimension of a scalar time series, *Physica D Nonlinear Phenomena, 110*(1-2), 43–50.

[98] **Kızılkaya, M**. (2012), Algorithm for FNN, retrivied from: http://www.mathworks.com/matlabcentral/fileexchange/37239-minimum-embedding-dimension/content/fnn_deneme.m

[99] **Rosenstein, M. T., Collins, J. J., De Luca, C. J.** (1992). A practical method for calculating largest Lyapunov exponents from small data sets, *Physica D Nonlinear Phenomena, 65*(1-2), 117–134.

[100] **Abarbanel, H. D. I., Brown, R., Kennel, M. B.** (1992). Local Lyapunov exponents computed from observed data, *Journal of Nonlinear Science*, *2*, 343 - 365.

[101] **Mccaffrey, D. F., Ellner, S., Gallant, A. R., Nychka, D. W.** (1992). Estimating the Lyapunov exponent of a chaotic system with nonparametric regression, *Journal of the American Statistical Association*, *87*(419), 682–695.

[102] **Gencay, R., Dechert, W. D.** (1992). An algorithm for the n Lyapunov exponents of an n-dimensional unknown dynamical system, *Physica D Nonlinear Phenomena*, *59*, 142–157..

[103] **Sun, Y., Wu, C. Q.** (2012). A radial-basis-function network-based method of estimating Lyapunov exponents from a scalar time series for analyzing nonlinear systems stability, *Nonlinear Dynamics*, *70*(2), 1689–1708,

[104] **Shintania,O., Linton, M.** (2004). Nonparametric neural network estimation of Lyapunov exponents and a direct test for chaos, *Journal of. Econometrics*, *120*, 1–33.

[105] **Dechert, W. D., Gencay, R.** (1992). Lyapunov exponents as a nonparametric diagnostic for stability analysis, *Journal of Applied Econometrics*, *7*,41–60.

[106] **Mohammadi, S.** (2009). Lyaprosen: MATLAB Function to Calculate the Largest Lyapunov Exponent, retrivied from:https://ideas.repec.org/c/boc/bocode/t741502.html

[107] **Kızılkaya, M.** (2013). Rosenstein Algorithm, retrivied from: http://www.mathworks.com/matlabcentral/fileexchange/38424-largest-lyapunov-exponent-with-rosenstein-s-algorithm/content/lyarosenstein.m.

[108] **Marwan, N.** (2014). MATLAB Cross Recurrence Plot Toolbox, retrivied from: http://tocsy.pik-potsdam.de/CRPtoolbox/, Potsdam Institute for Climate Impact Research, Potsdam, Germany.

[109] **Kirtley, J., Englebretson, S**. (2010). *MIT RLE Progress Report, Chapter 15: Electric Machinery,* retrivied from: http://www.rle.mit.edu/media-content/archive-progress-report/ Massachusetts, USA.

.

CURRICULUM VITAE

Name Surname: Sezen YILDIRIM ÜNNÜ

Place and Date of Birth: Eskişehir 30/04/1984

E-Mail: sezeny@itu.edu.tr

EDUCATION:

B.Sc.: **2006,** Istanbul Technical University – Electrical Engineering Department

M.Sc.: **2009,** Istanbul Technical University – Electrical Engineering Department

PROFESSIONAL EXPERIENCE AND REWARDS:

Visiting Scholar
Virginia Polytechnic Institue and State University **Washington DC USA**
October. 2013- May. 2014
Electrical Engineering Department in Falls Church

Research Assistant
Istanbul Technical University **Istanbul TURKEY**
December 2006 - Present
Electrical Engineering Department

REWARDS

2013: ***The Scientific and Technological Research Council of Turkey (TUBITAK)***

Scholarship for Visiting Scholars

2008: ***ABB***

Research Assistant Scholarship

JOURNAL PUBLICATIONS AND PRESENTATIONS RELATED WITH THE THESIS

- **Unnu, S. Y.,** Seker, S. (2014). Multiresolution Wavelet Analysis For Ferroresonance Phenomena on Power System. *Electric Power Components and Systems*, *42(6)*, 567-575.

- Akinci, T. C., Ekren, N., Seker, S., **Yıldırım, S.** (2013). Continuous wavelet transform for ferroresonance phenomena in electric power systems, *International Journal of Electrical Power and Energy Systems,* 44(1), 403–409..
- Akıncı, T. Ç., Ayaz, E., **Ünnü, S. Y.,** Şeker, S. (2014). A Review Study on Ferroresonance Phenomenon in Power Systems. In *International Conference on Technics, Technologies and Education,* Yambol, Bulgaria, 30 – 31 October. 2014,
- **Yıldırım, S.,** Bayram, D., Akıncı, T. Ç., Şeker, S. (2010). Continuous Wavelet Transform for Ferroresonance Phenomenon in Electric Power Systems. *In The Fifth International Symposium on Wavelets to the World Problem*, Istanbul Aydın University, Turkey, 7 – 8 June.

OTHER PUBLICATIONS, PRESENTATIONS

- **Unnu, S. Y.,** Erdem, L. (2012). Impacts Of Lighting Systems On Students: A Case Study. In *the 5th Balkan Conference on Lighting*, Belgrade, Serbia, 3 -6 October.
- Bayram, D., **Unnu, S. Y.,** Şeker, S. (2012). Lyapunov Exponent for Aging Process in Induction Motor. In the *10th International Conference Of Numerical Analysis And Applied Mathematics,* Kos Island, Greece, 19 – 25 September.
- **Unnu, S. Y**., Şener, F., Yener, A. K. (2011). The Role of Control Systems in Calculating Lighting Energy Performance of Buildings. In the *II. National Congress of Electrical Installation*, İzmir, Turkey, November.
- Şener, F., **Unnu, S. Y**., Yener, A. K. (2011). The Role of the Geographical Properties in Calculating Lighting Energy Performance of Buildings. In the II. National Congress of Electrical Installation, İzmir, Turkey, November 2011.
- **Unnu, S. Y**., Şener, F., Yener, A. K. (2011). Adaptation of EN 15193 Standard for Turkey, BEP-TR Methodology and Case Study Applications, *In The 27th Session of CIE,* Sun City, South Africa, 9 – 16 July 2011.
- Şener, F., **Unnu, S. Y**., Yener, A. K. (2011). Lighting Energy Performance Assessment Tools for building Certification Systems in Europe. *In The 27th Session of CIE,* Sun City, South Africa, 9 – 16 July 2011.
- Şener, F., **Unnu, S. Y**., Yener, A. K. (2011). Calculating Lighting Energy Performance of Buildings by BEP-TR Methodology – Several Examples. In *The Tenth. National Congress of Mechanical Engineering,* İzmir, Turkey, April.
- Bayram, D., **Yıldırım, S**., Akıncı, T. Ç., Şeker, S. (2010). Multi Resolution Wavelet Analysis for Fault Detection In Induction Motors. In *The Fifth International Symposium on Wavelets to the World Problem.,7- 8* June 2010, İstanbul, Turkey.
- **Yıldırım, S**., Enarun D. (2010). Design of an Emergency Lighting Fixture Using Light Emitting Diodes. In *CIE - 2010 Lighting Quality and Energy Efficiency,* Vienna, Austria, 14 - 17 March.

- **Yıldırım, S**., Kesler, M. (2009). The Utilization of LEDs in Automotive Industry and a Case Study in Turkey, Proceedings of Lux Europe, Istanbul, Turkey, 9 - 11 September.
- **Yıldırım, S**., Enarun D. (2009). Design of a Lighting Fixture for Using in Emergency Lighting (In Turkish)", In AYSEM, İzmir, Turkey, May.
- **Yıldırım, S**., Jazayeri, M., Erdem, L., Enarun, D. (2008).The Importance of Lighting Levels in Emergency Lighting (In Turkish). In *The Seventh National Lighting Congress*, Istanbul Technical University, Turkey, November.